
**DRAFT OF THE MODIS LEVEL
1B ALGORITHM
THEORETICAL BASIS
DOCUMENT VERSION
2.0 [ATBMOD-01]**



February 13, 1997

SAIC/GSC MCST Document

Prepared by:

Richard Barbieri
MODIS MCST Task Leader

Date

Reviewed by:

Harry Montgomery
MCST Algorithm Development Team

Shiyue Qiu
MCST Algorithm Development Team

Bob Barnes
MCST Algorithm Development Team

Approved by:

Bruce Guenther
MCST Manager

Vincent V. Salomonson
MODIS Science Team Leader

1. INTRODUCTION.....	3
1.1 DOCUMENT AND DATA PRODUCT IDENTIFICATION	3
1.2 THE MOD-01 DATA PRODUCT AND ITS ROLE IN MODIS DATA PROCESSING	4
1.3 STATEMENT OF DOCUMENT SCOPE.....	4
2. OVERVIEW AND BACKGROUND INFORMATION.....	4
2.1 EXPERIMENTAL OBJECTIVE	4
2.2 HISTORICAL PERSPECTIVE.....	5
2.3 INSTRUMENT CHARACTERISTICS.....	5
2.4 THE CALIBRATION TIMELINE.....	12
2.4.1 <i>Synthesis of Calibration Data and Schedule.....</i>	<i>12</i>
2.4.1.1 Preflight.....	12
2.4.1.2 Activation and Evaluation (A&E) Phase.....	13
2.4.1.3 Operational Phase.....	13
3. ALGORITHM DESCRIPTION.....	13
3.1 THE REFLECTED SOLAR BANDS	14
3.1.1 <i>The Basic Measurement Equation.....</i>	<i>14</i>
3.1.1.1 Effective Digital Counts.....	16
3.1.1.2 Radiance Responsivity.....	18
3.1.1.3 Calculation of B	20
3.1.1.4 Reflectance Responsivity.....	21
3.1.1.5 Uncertainty Estimate.....	22
3.1.2 <i>Product Flow in the Algorithm.....</i>	<i>24</i>
3.1.2.1 Programming Considerations.....	25
3.1.2.2 Quality Control and Diagnostics.....	25
3.1.2.3 Exception Handling.....	25
3.1.2.4 Output Product.....	26
3.2 THE EMISSIVE INFRARED BANDS.....	26
3.2.1 <i>Basic Measurement Equation.....</i>	<i>26</i>
3.2.1.1 The Master Curve Premise and Quadratic Calibration Equation.....	27
3.2.1.2 Conversion from MODIS Counts to Detector Preamplifier Output Voltage.....	30
3.2.1.3 The Calibration Transfer.....	31
3.2.1.4 Summary of the Calibration Parameters.....	31
3.2.2 <i>Uncertainty Analysis.....</i>	<i>32</i>
3.2.3 <i>Constraints, Limitations and Assumptions.....</i>	<i>34</i>
3.2.3.1 Detector 1/f Noise Correction.....	34
3.2.3.2 Instrument Spurious Source Corrections.....	35
3.2.4 <i>Practical Considerations.....</i>	<i>36</i>
3.2.4.1 Programming Considerations.....	36
3.2.4.2 Quality Control and Diagnostics.....	36
3.2.4.3 Exception Handling.....	36
3.2.4.4 Output Product.....	37
3.3 THE SPECTRORADIOMETRIC CALIBRATION ASSEMBLY (SRCA).....	37
3.3.1 <i>The Radiometric Mode.....</i>	<i>37</i>
3.3.2 <i>The Spectral Mode.....</i>	<i>38</i>
3.3.3 <i>The Spatial Mode.....</i>	<i>38</i>
3.4 VICARIOUS CALIBRATION.....	39
3.4.1 <i>An Overview.....</i>	<i>39</i>
3.4.1.1 The Fundamental Concept.....	39
3.4.1.2 Vicarious Calibration and the MCST Strategy.....	41
3.4.1.3 Uncertainty Estimates.....	42
3.4.2 <i>Practical Considerations.....</i>	<i>42</i>
3.4.2.1 Programming Considerations.....	42
3.4.2.2 Vicarious Calibration and Validation.....	42
3.4.2.3 Quality Control, Diagnostics and Exception Handling.....	42
3.5 CALIBRATING THE ENGINEERING TELEMETRY DATA	42
3.5.1 <i>Theoretical Description.....</i>	<i>42</i>
3.5.1.1 Mathematical Description of Algorithm.....	42
3.5.1.2 Uncertainty Estimates.....	43

3.5.2 *Practical Considerations*.....43

 3.5.2.1 Quality Control and Diagnostics.....43

 3.5.2.2 Exception Handling.....43

 3.5.2.3 Output Product.....43

4. ISSUES TO BE ADDRESSED43

5. APPENDIX A: PEER REVIEW BOARD ACCEPTANCE REPORT.....45

6. APPENDIX B: MODIS SPECTRAL BANDS SPECIFICATION46

7. APPENDIX C: KEY MODIS REQUIREMENTS.....47

8. APPENDIX D: ACRONYMS AND ABBREVIATIONS48

9. APPENDIX E: REFERENCES.....50

10. APPENDIX F: LEVEL 1B OUTPUT FILE SPECIFICATION.....52

11. APPENDIX G: SPURIOUS RADIANCE CONTRIBUTION SOURCES SUMMARY.....68

The authors of this document are:

Richard Barbieri¹, Harry Montgomery², Shiyue Qiu¹, Bob Barnes¹, Daniel Knowles Jr.¹, Nianzeng Che³, and I. Larry Goldberg³.

1) General Sciences Corporation, Seabrook, MD 20706

2) NASA, Goddard Space Flight Center, Greenbelt, MD 20771

3) Swales and Associates, Inc., Beltsville, MD 20705

1. INTRODUCTION

The Moderate Resolution Imaging Spectroradiometer (MODIS) is the cornerstone instrument for both the AM-1 and PM-1 series of spacecraft; AM-1 (10:30 AM descending node) is scheduled for launch in June 1998 and PM-1 (2:30 PM ascending node) is scheduled for launch in 2000. MODIS continues the lineage of the Coastal Zone Color Scanner (CZCS), the Advanced Very High Resolution Radiometer (AVHRR), the High Resolution Infrared Spectrometer (HIRS), and the Thematic Mapper (TM).

MODIS is a passive, imaging spectroradiometer carrying 490 detectors, arranged in 36 spectral bands, that cover the visible and infrared spectrum. It is a high signal-to-noise instrument designed to satisfy a diverse set of oceanographic, terrestrial, and atmospheric science observational needs. It will make global moderate-resolution narrow-band radiance observations over 36 spectral regions; it does so by using a continuously rotating, double-sided, scan mirror which views the earth, internal calibrators, and space at 20.3 rpm; that is, one side of the mirror traverses 360 degrees every 1.477 seconds. The EOS AM-1 spacecraft will be in a near polar, sun-synchronous orbit at an altitude of 705 km. The Earth swath is perpendicular to the ground track and subtends a scan angle of 110 degrees. There are three calibrator systems inside the MODIS instrument: a Solar Diffuser (SD) with a Solar Diffuser Stability Monitor (SDSM), a Spectroradiometric Calibration Assembly (SRCA); and a Blackbody (BB). In addition there is a Space View (SV) port that is used to provide a zero reference.

The MODIS Characterization Support Team (MCST), working under the direction of the MODIS Team Leader, has the primary responsibility for developing the characterization and calibration algorithms for the MODIS instruments. This responsibility includes the development of the MODIS Level 1B Algorithm Theoretical Basis Document (ATBD) and the design and development of the L1B code.

The primary MCST products are top of the atmosphere radiance and reflectance scales and offsets. Furthermore MCST identifies the nadir pixel and geolocation information, and provides uncertainty and scene contrast indices. MCST designs and develops the L1B code; it is this code that produces the products listed above. The code is founded upon the understanding of the instrument as expressed and documented in the ATBD. Appendix F contains the entire L1B output file specification.

1.1 Document and Data Product Identification

The parent documents of this document are [EOS, 1994] and [Salomonson, 1994]. Previous relevant publications include [Guenther *et al.*, 1995], [King, 1994], [Weber, 1993], [SBRC, 1993], and [SBRC, 1994a]. Other applicable documents are listed in the references section.

This is a summary document. The algorithms described will be used for the Version 2.0 software of the MODIS Level 1B processing. There are accompanying detailed support documents which, when taken together with this summary document, comprise the entire Version 2.0 of the MODIS Level 1B Algorithm Theoretical Basis Document (ATBD).

The L1B Version 2.0 code will be delivered at the end of April 1997 well before analysis of the ProtoFlight Model (PFM) data is completed. The 2.1 version of the software, planned for at-launch use, is expected to contain better understanding of the instrument based on more complete analyses and interpretations of PFM data. After launch new algorithms and software will be developed in response to the inflight behavior of the MODIS instrument.

1.2 The MOD-01 Data Product and its Role in MODIS Data Processing

The MOD-01 calibration data product results from the application of the formulas and corresponding uncertainties described in this document and the accompanying support documents. The support documents present the details of how the instrument data are transformed from counts to:

- (1) radiances, reflectance cosine theta values, and effective digital numbers, DN , for the solar reflecting bands,
- (2) radiances for the emissive bands,
- (3) changes from prelaunch calibration of center wavelengths for the solar reflecting bands,
- (4) relative spatial shifts of the pixels along scan and the bands along track.

Items (1) and (2) are the focus of this document and also the focus of the online production processing efforts. They will be produced for every granule at the DAAC. Items (3) and (4) are done offline from the production processing. They will be produced with the Compute Resources of MCST (CROM).

1.3 Statement of Document Scope

This document describes the physical and engineering understanding of how MODIS will operate in space and it addresses the equations used by the L1B software that, in turn, generate the MODIS MOD-01 data product. It is a summary document that presents the formulae and error budgets used to transform MODIS digital counts to radiance and reflectance. Furthermore this document describes the MODIS calibration and validation process. This document also provides references to documents containing more complete derivations of results and to documents that explain the implementation of these algorithms as computer programs.

Geolocation information is assumed within the L1B algorithm; a separate ATBD exists for the MODIS geolocation algorithms [*Wolfe et al.*, 1995].

The MODIS Level 1B Data Product Specification is provided in Appendix F. Data flow diagrams, program module descriptions and metadata descriptions are described fully in the *MODIS Level 1B Software Design Document* [*Hopkins et al.*, 1995b]. Summary data flow diagrams are provided for the Reflected Solar and Emissive infrared bands algorithms in those sections.

The approach for developing offline products for data sets from the SRCA calibrators and the engineering data is described in sections 3.3 and 3.5. The basic strategy for making improvements to the product corresponds to improved understanding of the sensor performance. The contributions to this process expected from vicarious calibration is discussed in section 3.4. There are numerous areas where Engineering Model (EM) test data are not adequate to describe the PFM performance. Specific instances where there is uncertainty regarding sensor performance are reviewed in section 4. There are areas that MCST will watch carefully during the PFM thermal vacuum test program and these will be analyzed.

2. OVERVIEW AND BACKGROUND INFORMATION

2.1 Experimental Objective

The MODIS Level 1B on-line data products are Top of the Atmosphere (TOA) radiance and reflectance; these will be radiometrically corrected and fully calibrated in physical units at the instrument spatial and temporal resolutions. The MODIS instrument key calibration and characterization requirements are listed in Appendix C. The algorithms described in this ATBD are designed to meet those requirements and, therefore, the science needs of the MODIS science community. A review of the current strategy for the at-launch calibration for MODIS is given by [Guenther *et al.*, 1996].

2.2 Historical Perspective

Documents directly preceding the MODIS L1B ATBD 1995 were titled both as ATBD and as Calibration Plans. The first was the MODIS Level 1 Geolocation, Characterization and Calibration Algorithm Theoretical Basis Document, Version 1 [Barker *et al.*, 1994]; it corresponds to the MCST Beta-2 code delivery. The next was the MODIS Calibration Plan [Team *et al.*, 1994] and correspond to the MCST Beta-3 code delivery. The third in the series was MODIS Level 1B Algorithm Theoretical Basis Document [MOD-01] [Guenther *et al.*, 1995] which corresponds to the MCST Version 1.0 delivery. This document is the fourth in that direct line. Other relevant documents are listed in Appendix E

2.3 Instrument Characteristics

MODIS has 36 spectral bands with center wavelengths ranging from 0.412 μm to 14.235 μm ; these are listed in Appendix B. Two of the bands are imaged at a nominal resolution of 250m at nadir, five bands are imaged at 500m, and the remaining bands at 1000m. Bands 13 and 14 each have two gain settings, 13 low, 13 high, 14 low, and 14 high, telemetered from the instrument. All bands are telemetered at 12 bits.

Scene radiant flux reflects from the double sided, beryllium scan mirror, that is continuously rotating at 20.3 rpm with a period maintained to ± 0.001 sec so as to control scan to scan underlap. It is oval shaped, 21 cm wide (the axis of rotation) and 58 cm long. The mirror is nickel plated and coated with silver for high reflectance and low scatter over the broad spectral range of the sensor. The reflectivity of the each side of the scan mirror is a function of the AOI and will be accounted for in the algorithms.

Energy from the scan mirror then impinges upon the Afocal telescope assembly fold mirror that, in turn, reflects the energy into a plane perpendicular to the scan plane so as to cancel polarization between the scan mirror and the fold mirror. The energy then strikes the primary mirror (the entrance pupil), goes through a field stop and then onto the secondary mirror. The mirrors are made of Zero-Dur low expansion substrates with protected silver coatings. The individual mirror elements are mounted onto a graphite-epoxy structure to maintain alignment of the elements. The assembly must maintain optical performance over a temperature range $\pm 10^\circ\text{C}$. Immediately after the secondary mirror is a dichroic beamsplitter assembly (consisting of three beamsplitters) that directs the energy through four refractive objective assemblies and then onto the four focal plane assemblies (FPAs) with their individual bandpass filters. The beamsplitters are used to achieve spectral separation, dividing the MODIS spectral domain into four spectral regions: visible (VIS) (0.412 to 0.551 μm), near infrared (NIR) (0.650 to 0.940 μm), short wavelength/medium wavelength infrared (SWIR/MWIR) (1.240 to 4.565 μm), and long wavelength infrared (LWIR) (6.715 to 14.235 μm). Dichroic 1 uses a ZnSe substrate and reflects the entire VIS, NIR region while transmitting the balance of the scene energy to 14.235 μm . Dichroic 2 uses a BK-7 substrate

and reflects energy to the bands between 0.400 μm and 0.600 μm . Dichroic 3 also uses a ZnSe substrate and reflects energy to bands between 1.24 μm and 4.515 μm . Out-of-spectral-band rejection is accomplished through blocking filters on both bandpass filters and dichroics.

Each spectral region has an objective lens assembly for imaging scene energy onto the corresponding focal plane. On each focal plane are rows of detectors aligned in the along track direction so as to image 10km in the along track direction of the scan. Consequently there are 10 detectors along track in the 1000m bands, 20 detectors along track in the 500m bands, and 40 in the 250m bands.

Spectral separation occurs at the FPAs with dielectric bandpass filters for each band. These filters are deposited on glass substrates; in some cases two filters are deposited on a single substrate. The filter substrates are mounted to a mask common substrate, one per FPA. The mask provides some spectral out-of-band blocking as well as masking for the field-of-view of the detectors. Low residual polarization sensitivity is required for bands between 0.43 μm to 2.2 μm the requirement for less than 2% polarization between 0.43 μm to 2.2 μm is achieved by using silver coated mirrors, crossed scan and fold mirrors and a compensator plate in the NIR objective.

The VIS and NIR FPAs operate at ambient temperature and are covered by photovoltaic silicon hybrids for low noise readout and excellent transient response performance. A HgCdTe photovoltaic detector hybrid is used on the SWIR/MWIR FPA, and one is also used for all bands out to 10 μm on the LWIR FPA. The LWIR FPA also includes six band photoconductive HgCdTe detectors for wavelengths beyond 10 μm because these offer better performance at 85K at wavelengths greater than 10 μm .

The passive radiative cooler assembly is designed to passively cool the SWIR/MWIR and LWIR focal planes to 85K. The cooler requires a 170 by 115 degree clear field of view to space and employs three stages of cooling to achieve the operating temperature of 81K. A 4K margin allows for potential degradation over the mission life and temperature control. The cold stage assembly houses the SWIR/MWIR and LWIR focal plane assemblies. The intermediate cooler window will operate at approximately 137K on orbit.

There is an analog signal processing electronics unit and an analog-to-digital conversion electronics unit to provide the primary clocks and bias voltages for all the photovoltaic detectors, preamplification of the LWIR photoconductive detectors, and conversion of the analog signals to 12 bit digital signals.

As the MODIS mirror scans, energy from several On-Board Calibrators (OBC) is reflected into the telescope (see Figure 1). Both sides of the rotating scan mirror are used. As the scan mirror rotates, the following events occur (see Figure 2):

On-Board Calibrators in MODIS Scan Cavity

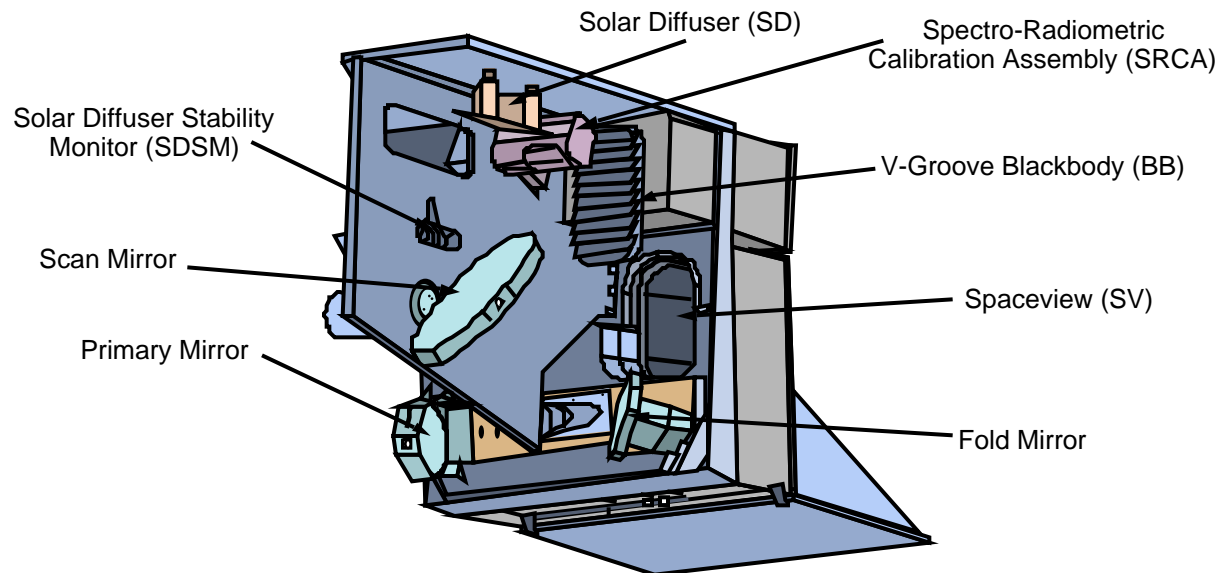


Figure 1. MODIS views a sequence of On-Board Calibrators.

(1) The mirror scans the SD. When the AM platform is near the north pole on the day side of the terminator and the SD door is open, the SD is fully illuminated by the Sun for approximately two minutes. The angle of incidence (AOI) of light from the diffuser which penetrates to the detectors ranges from 50.9 to 49.6 degrees. During this period of time the SDSM is operated. The SDSM alternately looks at the sun through an attenuation screen and the SD. Sunlight is scattered off of the SD and corrected for SD degradation using the SDSM; this process is used to track the radiance calibration stability of the reflected solar bands.

(2) The mirror scans the SRCA. The SRCA is used to track changes in the radiometric calibration of MODIS through launch, to characterize the limits of within-orbit changes in responsivity for the reflected solar bands, to determine the center wavelength for these bands, and to track the along-scan shift in Earth location for each detector and the along-track shift for each of the 36 bands. The AOI range of the SRCA scan is 38.4 to 38.1 degrees. Sources within the SRCA are activated by ground command.

(3) The mirror scans the BB. The BB provides one point on the calibration curve for each detector of the emissive bands. The BB is viewed and used for each scan line. The BB temperature is approximately isothermal with respect to the scan cavity. The AOI range of the BB is 27.3 to 26.6 degrees.

(4) The mirror scans the SV port. This view provides the zero reference points on the calibration curves for all 36 spectral bands. The SV is viewed and used for each scan line for each band. A few times per year the moon will be visible through the SV. During those times the moon will provide a radiance source for vicarious calibration rather than a zero radiance reference. The SV is used for scan mirror AOIs 11.6 to 10.9 degrees.

(5) The mirror scans the EV port; the view of earth subtends 110-degrees in the scan plane perpendicular to the along-track direction. The remainder of the cycle is used to format science and engineering data, execute commands, and perform DC restore operations. The AOI range of the EV is 10.5 to 65.5 degrees.

Sector	# Frames Available	# Frames used in the L1B Code	AOI
SD	50	the central 15	50.9-49.6
SRCA	15	15	38.4-38.1
BB	50	the central 15	27.3-26.6
SV	50	the central 15	11.6-10.9
EV	1354	1354	10.5-65.5

The order of the sectors described above is the order of the data in the Level 0 data stream and is the order of the scan mirror viewing; this is shown in Figure 2.

The targets for the SV and the EV are in the far field of the sensor and are in focus. The targets for the SD, SRCA, and the BB are in the near field and will not be in focus.

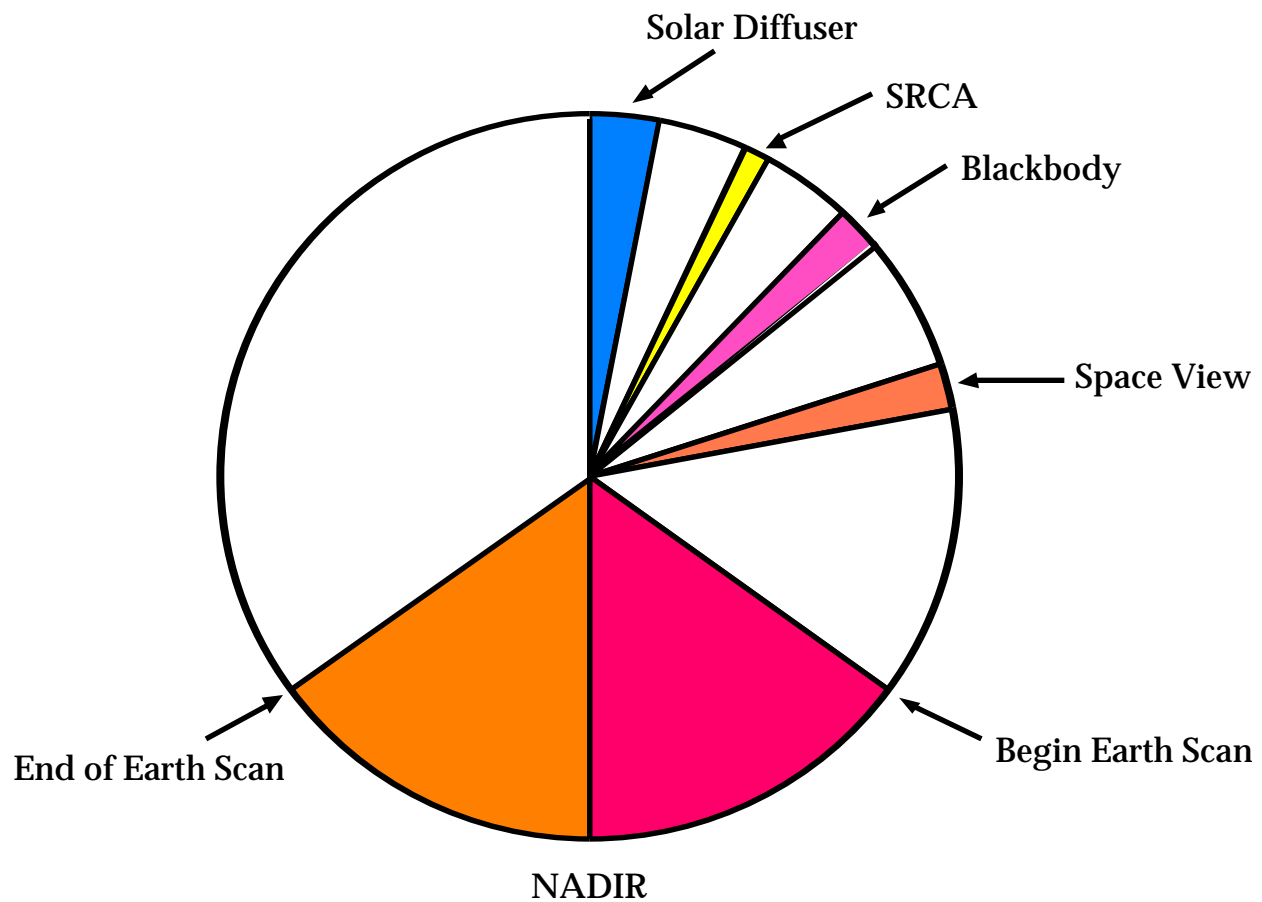


Figure 2. As the MODIS Scan Mirror rotates, each side scans the Solar Diffuser, the Spectro-Radiometric Calibration Assembly, the blackbody, Space-and the Earth.

The ground track direction is designated as the +x direction; in the ground projection point of view looking in the +x direction, the scan (which takes 1.471sec) moves from right to left orthogonal to the track direction. A swath (also known as a scan line) is 2200km long and 10km wide at NADIR and orthogonal to the track direction. A swath contains 1354 frames per scan. A frame size is 1km

in the scan direction and 10km in the track direction at NADIR. The paddle wheel scanner has a bowtie characteristic at the scan edges, where the scan enlarges to 3km by 20km with a rotated field of view. For bands 8-36 the intrinsic detector (pixel) size matches by 1km ground instantaneous field of view (IFOV). There are 10 detectors in the track direction for these 1km bands.

The 500m bands (bands 3-7) have detector sizes that correspond to an IFOV of 500m by 500m. There are 20 detectors in the track direction, and each detector is sampled two times within a frame.

The 250m bands (bands 1 & 2) have detector sizes that correspond to an IFOV of 250m by 250m. There are 40 detectors in the track direction and each detector is sampled four times within a frame.

In a given frame, the ordering of the ten pixels is such that IFOV₁ is at the leading edge of the scan in the track direction and IFOV₁₀ is at the trailing edge of the scan. A corresponding numbering scheme is used for the 500m and 250m bands.

THE SOLAR DIFFUSER AND SOLAR DIFFUSER STABILITY MONITOR

The SD is a full aperture, end to end calibrator used to provide a measurement of sunlight for calibration of reflected solar bands. The diffuse surface is made from space grade Spectralon because it has high reflectance in the VIS-NIR-SWIR regions and it has a near Lambertian reflectance profile. Once per orbit at the North pole when the diffuser door is open, solar energy strikes the diffuser. Knowledge of the reflectance properties of the diffuser and the sun angle allows a computation of the radiance of the diffuser for checking radiometric calibration of the reflected solar bands. Data accumulated when the solar diffuser is illuminated is accepted as valid when the instrument is on the dark side of the terminator as this limits the amount of stray light entering the instrument through the Earth view port during the calibration interval. Because of the mounting of the SD, radiance levels for most bands will be near the upper end of the dynamic range. High gain bands saturate at much lower radiances and for these bands an 8.5% transmission screen can be deployed in the SD viewport.

Solar Diffusers usually deteriorate on orbit due to sunlight. MODIS design includes a solar diffuser stability monitor to track the reflectances of the SD. The SDSM consists of a spectralon surface integrating sphere and a pointing mirror. A 2 percent transmission screen is installed at the SDSM aperture. The pointing mirror alternately points at the attenuated direct sunlight, the sunlight scattered by the SD and a dark housing. These sources illuminate the SDSM integrator which is fitted with 9 silicon photodiode detectors. The spectral bandpass of these detectors approximate nine MODIS bands between 0.4 μm to 0.9 μm . The dark housing signal is used to correct for silicon photodiode detector dark signal drift.

The SD/SDSM processing is done off-line.

THE SRCA

The SRCA is an end-to-end, partial aperture calibrator. It operates in three modes: spectral, radiometric, and spatial. In the spectral mode, instrument spectral response from 0.4 μm to 2.1 μm is tracked. In the spatial mode, instrument spectral band registration for all bands in both scan and track directions is tracked by using well defined reticules. The radiometric mode provides a radiometric reference level using a lamp to allow transfer of ground calibration to in-orbit calibration using the diffuser. In the radiometric mode, the instrument response from 0.4 μm to 2.1 μm is tracked compared to prelaunch behavior with one 1 watt and up to three 10 watt lamps.

The SRCA design uses internal systems to track the SRCA behavior for the spectral and radiometric operating modes. A didymium glass absorption filter and separate detectors are used to establish the SRCA wavelength scale. The output collimator for the SRCA is atelescope, and a silicon photodiode detector mounted in the central obscuration of the collimator. This detector is not temperature compensated but can be used to track changes in the SRCA spectral source signal strength through a spectral calibration sequence. A temperature controlled silicon photodiode detector is mounted in the SRCA integrator source assembly which can be used for operating the lamps in a radiometrically atable feedback mode or for tracking lamp output when the lamps are operated in a constant current mode.

The SRCA processing is done off-line.

THE BLACK BODY

The V-groove BB is a full aperture radiometric calibration source for the MWIR and LWIR bands. It provides a known radiance source and is also used in the DC restore operation. The requirement for calibration forces the need for temperature uniformity and a high effective emissivity (>0.992). The BB is calibrated in comparison to the primary infrared calibration (the blackbody calibration source, BCS) during the thermal vacuum testing.

The scan cavity is designed to be at constant temperature throughout and the BB will float at the scan cavity temperature (nominally 273K). The BB can be heated and controlled at 315K. The BB temperature is monitored but not controlled. Twelve thermistors are embedded near the front radiating surface to measure the temperature and infer the temperature gradient along the surface. These thermistors are traceable directly to a NIST standard temperature scale.

The BB processing is done on every granule, is an integral part of the emissive INFRARED calibration and is done on-line in the DAAC

THE SPACE VIEW

This is an opening in one of the electronic modules which permits a direct view of cold space. It is meant to provide the sensor response to a zero input radiance source. This is a full aperture calibrator that is viewed once per scan by all bands. For the emissive infrared bands it provides the second calibration point for a linear calibration as required by the BB. This calibration is used to establish the gain and zero-offset of the emissive infrared detectors. The possibility of a lunar calibration of the reflective bands on a time scale of 2-5 years is provided by the fact that the Moon passes through the SV port two to six times a year at approximately 2/3rds of full moon. The Space View can also be used to obtain the zero offset for the detectors in the reflected solar part of the spectrum.

The Level 1B Version 2.0 code is written in a way which partitions the bands into reflected solar and emissive infrared.

The Reflected Solar Bands (1-19 and 26)

The MODIS design monitors on-orbit detector responsivity of the reflected solar bands by periodically opening a protective door over the MODIS forward enclosure aperture and allowing solar radiation to illuminate a Spectralon™ SD panel. In principle, the radiance of the illuminated SD is directly proportional to the solar constant adjusted for the Earth-Sun distance, the transmittance of an optional attenuation screen, the reflectance of the diffuser, and the cosine of the solar incidence angle. Before launch, sources traceable to NIST standards define the absolute radiance calibration of the MODIS VIS, NIR, and SWIR reflected solar bands; on-orbit, the

radiance scale is transferred to the SD/SDSM system. The MODIS radiance calibration is monitored during the A&E phase with the prelaunch calibrated SRCA. The SD assembly provides two known radiance levels for bands 1-7, and bands 17-19 with direct views of the SD; and for all reflective bands with an attenuation screen limiting the SD radiance. The transmittance of the SD screen is a nominal 8.5% but has a measured variation that is a function of solar incidence and MODIS-view geometry. The SDSM will enable MODIS to perform an estimate of the Earth-scene bidirectional reflectance factor (BRF).

The calibration coefficients for the MODIS reflected solar bands are called responsivities and carry units of counts per unit radiance and counts per unit reflectance. These responsivities are determined in the laboratory during instrument characterization by observation of a calibration standard. During A&E, the radiance responsivity of MODIS is monitored by the SRCA. After A&E, changes in the responsivities of the reflected solar bands are monitored with the SD looking at the sun. However the SD is not in the same optical path when MODIS measurements are made of the Earth exiting radiance. This means that expected temporal changes in MODIS responsivities must be distinguished from inevitable changes in the diffuser plate over mission lifetime. The first step in making the separation is to use the ratioing radiometer, the SDSM. Its purpose is to monitor the changes in the reflectance of the diffuser by alternately viewing the sun and the diffuser in a repeating sequence throughout any MODIS solar measurement event. The SDSM alternating sequence yields the ratio of the radiant flux from the two sources. Along with other techniques, the linearity of the SDSM will be checked on orbit by monitoring the ratio of the SDSM's measurements of the flux from the SDSM diffuser screen (8.5% nominal transmittance) to measurements of the sun directly.

For the purpose of monitoring changes in the radiance responsivities of the reflected solar bands, the sun is assumed to be a source of constant radiance. This radiance is combined with measurements of the solar diffuser reflectance and an estimate of the earth-sun distance to provide a reference radiance from the diffuser. The long-term repeatability of MODIS will be tracked by monitoring this reference radiance.

In addition to its function as a radiometer that measures the Earth exiting radiance, MODIS can also be paired with the SD/SDSM to act as a reflectometer. In this measurement mode, the SD and the earth are both reflecting plates, and MODIS becomes a ratioing radiometer (the transfer instrument between the two plates). In this role, MODIS is assumed to have a linear response. Once corrections are made for the earth-sun distance, the solar infrared radiance is eliminated from the measurement because the earth and SD are illuminated by the same source and the source infrared radiance cancels in the ratio. Prelaunch measurements of the reflectance responsively are used for the MODIS reflectance measurements, and the SDSM monitors the on-orbit changes in the reflectance of the solar diffuser.

The Emissive Infrared Bands (20-25 and 27-36)

The MODIS Emissive Infrared Bands consist of the photovoltaic (PV) detectors (Bands 20-25, and 27-30), and the photoconductive (PC) detectors (Bands 31-36). The same basic linear algorithm will be applied to both detector types, though the PV detector response to increasing flux levels is expected to be nearly linear, and the PC detector response is expected to be more nonlinear, requiring a quadratic response function basis. Thermal vacuum tests will demonstrate whether it is necessary to add a nonlinear term to the basic linear calibration equation to achieve the MODIS required calibration accuracy.

Each MODIS emissive infrared detector has an output consisting of a small signal superimposed on a large, variable background. The calibration process is to isolate the Earth view signal from the background. The calibration coefficients for the MODIS emissive infrared bands are provided as the system gain, background radiation and system nonlinearity if necessary. The system non-

linearity is measured prelaunch, and the system gain and background are measured in-flight by observing the space as the zero reference and the blackbody as its OBC.

The BB will be calibrated prelaunch through a careful mapping of the instrument response to the laboratory Blackbody Calibration Source (BCS), which produces precisely controlled radiance outputs traceable to NIST temperature standards. During the postlaunch, the BB parameters will be adjusted through the vicarious calibration (or cross calibrations with the other instrument measurements).

The calibration procedure within the LIB emissive algorithm has three parts: (1) the calibration transfer from BCS to the OBC blackbody and system nonlinearity measurement in the laboratory, (2) the on-line calibration process which involves the calculation of the system gain and background radiation using BB and SV measurements to obtain the EV radiance and its radiometric uncertainties, and (3) the off-line calibration process which involves the spacecraft maneuver to update the scan mirror reflectivity change, and vicarious calibration to update the calibration parameters estimated from the BCS transfer, as well as investigating special effects, performing Quality Assurance and trending/monitoring functions.

2.4 The Calibration Timeline

2.4.1 Synthesis of Calibration Data and Schedule

The primary calibration at launch is derived from the prelaunch calibration program. The MODIS response to the SRCA in each mode is obtained about the same time the sensor is calibrated. The BB emissivity will be tuned so the BB and the BCS provide the same calibrations for the emissive infrared bands.

When on orbit, changes in band coregistration inferred from the SRCA spatial mode will be incorporated with the data set (metadata) directly. Changes in band spectral registration inferred from the SRCA spectral mode will be compared with thermal vacuum spectral changes and incorporated directly into the metadata when those changes are consistent. When the on orbit changes are not consistent with thermal vacuum data the ground values will be included in the data sets and MCST will study sources of inconsistency.

In the emissive infrared bands, calibration will be provided on scan line by scan line basis automatically through BB and SV observations. Later, vicarious calibration measurements will be used to tune the BB temperature sensors.

In the reflected solar bands, prelaunch calibration will be used. Changes in this calibration will be tracked based on measurements from the SD/SDSM system. Changes in the at launch radiometric scale may be derived from vicarious calibration studies.

Throughout the entire lifetime of MODIS the calibration data will be trended, compared, and statistically analyzed to establish their credibility.

The MODIS processing system depends on a large number of instrument calibration and characterization parameters. Any process to change them over time will be reviewed with the MODIS Science Team.

2.4.1.1 Preflight

During sensor calibration tests, the OBCs will be characterized to establish an accurate comparison between ground sources and the OBCs. Preflight radiometric calibration of the MODIS will rely on a large spherical integrating source (SIS) for the VIS, NIR, and SWIR bands; a full aperture blackbody calibration source (BCS) will be used for MWIR and LWIR bands. These two sources will be separately calibrated with standards traceable to NIST primary standards. The BCS is traceable to NIST through temperature scales. Reflectance calibration will be accomplished by accurate measurement of the SD and a full aperture blackbody calibration source (BCS) will be used for the radiance calibration of the MWIR and LWIR bands.

Preflight spectral characterization is based on relative spectral response measurements made with a double grating monochromator. Preflight geometric characterization will also include band-to-band registration and instantaneous field of view (IFOV) determination.

Radiometric calibration will be accomplished using the SBRS 100 cm diameter SIS which will be validated via measurements using the NIST transfer radiometer. The Solar Diffuser Bi-Directional Reflectance Distribution Function (BRDF) will be accurately measured using the SBRS scatterometer which will be compared to scatterometers at GSFC, NIST, the University of Arizona and the University of Rochester in a Round-Robin measurement series using reference samples.

2.4.1.2 Activation and Evaluation (A&E) Phase

This phase covers approximately the first six months of operation for MODIS. The sensor turn on will occur about 1-2 days after nominal orbit is reached. The turn on will provide useful data for bands 1-19, except bands 5, 6, and 7. The radiometric calibration will initially be the prelaunch value. Regular measurements with the SD will start immediately. During this phase the operation, repeatability, and stability of the MODIS OBCs and the techniques developed to use them will be verified. Data trending, comparisons, and statistical analyses will be performed to improve instrument characterization and calibration.

When the OBC stability and performance have been verified, the SD measurements will be incorporated into the degradation algorithm automatically.

The cooler door will be operated about 45 days into mission operations. The BB and SV will be used for the emissive infrared calibrations immediately, based on the BB effective emissivity determined during system prelaunch thermal vacuum testing.

Vicarious calibration measurements will be used to validate the sensor product at Level 1B. Coincident measurements will be compared to the data product to validate the characterization and calibration of MODIS. Results of these comparisons will be presented to the Science Team and Team leaders for their review and recommendations. Responsibility for incorporation of changes due to vicarious calibration is with the MCST Leader, reporting to the MODIS Science Team Leader.

2.4.1.3 Operational Phase

From six months after launch until the end of the MODIS mission, OBC monitoring and trending, and vicarious data will be primary sources of information in the validation of the calibration coefficients. The techniques and the use of the moon for calibration are discussed in Section 3.4.

3. ALGORITHM DESCRIPTION

MODIS senses radiant flux at the top of the atmosphere at the MODIS aperture and records this flux as counts; the L1B code transforms the counts into radiance and reflectance. The sensed radiant flux may be partitioned into two components: reflected solar (includes wavelengths up to about 2.3 μm) and emissive infrared (greater than 2.3 μm). The next two subsections, 3.1 and 3.2, present a discussion of the equations used in the L1B code and a discussion of the calibration process for the reflected solar bands and the emissive infrared bands. The two algorithms discussed in the next two sections are the connecting links between the characteristics of the instrument, the data products, and their associated uncertainties. The reflected solar bands are numbered 1-19 and 26; the emissive infrared bands are numbered 20-36 excluding 26. See Appendix B.

3.1 The Reflected Solar Bands

3.1.1 The Basic Measurement Equation

MODIS carries the prelaunch laboratory calibration of the reflected solar bands to the scene that it views on orbit. For radiances from these bands, the basic measurement equation is

$$L_{EV,B,D} = \frac{DN_{EV,B,D}}{F_{VC,L,B} L_{B,D}} \quad (1)$$

where

B = Band

D = Detector

$L_{ev,B,D}$ = Spectral radiance from the Earth scene

$DN_{ev,B,D}^*$ = Radiance calibration factor from vicarious data

$F_{VC,L,B}^*$ = Radiance responsivity from the calibration of MODIS

$L_{EV,B,D}$ is the band-averaged spectral radiance of the scene, averaged over the wavelengths within which the detector has a significant quantum efficiency.

$$L_{ev,B,D} = \frac{\int_{\lambda_1}^{\lambda_2} L_{\lambda,ev} R_{\lambda,B} d\lambda}{\int_{\lambda_1}^{\lambda_2} R_{\lambda,B} d\lambda} \quad (2)$$

where

$L_{ev,B,D}$ = the spectral radiance of the Earth scene at wavelength

$R_{\lambda,B}$ = the relative spectral response at wavelength

λ_1 and λ_2 = the wavelength range over which the detector has a significant quantum efficiency

The effective digital counts, $DN_{ev,B,D}^*$, are the raw counts from MODIS, corrected for instrument characteristics determined during laboratory calibration and characterization. The effective digital counts correct for on-orbit differences from the laboratory conditions during calibration. For example, there is a correction for the difference between the temperature of the focal plane on orbit and that during calibration. These corrections are discussed in Section 3.1.2

The radiance calibration factor from vicarious data, $F_{vc,L,B}$, is a means of incorporating the results of lunar-, aircraft-, and ground-based measurements into the calibration of MODIS on orbit. This factor is applied to the calibration of MODIS that is derived from prelaunch measurements in the laboratory and subsequent measurements from onboard calibrators while on orbit.

The radiance responsivity, $R_{L,B,D}^*$, is the internally-generated calibration factor for MODIS. This factor has three components. The first comes from the prelaunch radiometric calibration in the laboratory. The second comes from measurements that monitor relative changes in the responsivity of MODIS during the time interval between the laboratory calibration and the start of on-orbit operations, that is, during the transfer to orbit. And the third comes from measurements to monitor relative changes in the responsivity of the instrument during the lifetime of the mission. For MODIS, there is only one absolute measurement of responsivity. This is the laboratory calibration. The two other components of the responsivity are measures of the relative changes in responsivity.

For the first factor, the laboratory calibration uses an integrating sphere as a known radiance source to calculate the responsivity of each detector at several radiance levels

$$R_{cal} = \frac{DN_{cal}^*}{L_{cal}} \quad (3)$$

and R_{cal} is represented as a fitted curve of the instrument digital counts to a set of calibration radiances.

For the second factor, the best estimate of the fractional change in responsivity during the transfer to orbit, ΔR_{tto} , is estimated from measurements from several sources. There is no procedure to automatically apply the transfer to orbit correction. Within MODIS, the SRCA will monitor instrument changes. In addition, initial measurements from the SD/SDSM will provide further evidence. Combined with measurements from lunar and other vicarious measurements, these data will be used to obtain an understanding of the instrument responsivity at the start of on-orbit operations. Only then will the transfer to orbit correction, ΔR_{tto} , be applied.

For the third factor, changes in the responsivity of the reflected solar bands are monitored after the start of on-orbit operations. During A&E, MODIS will make an initial set of solar measurements with the SD/SDSM. At this time, the radiance scales for the reflected solar bands will be transferred to the solar diffuser (Veiga et al., 1996).

For these and subsequent solar measurements, the solar diffuser will provide a reference radiance that is paired with the digital counts from the instrument to provide DN_{solar}/L_{solar} . During initial on-orbit operations, this ratio will be measured frequently, that is, more than once daily. As the

change in the instrument responsivity becomes understood, the interval between measurements will be increased. However, the measurement frequency will remain such that changes from one to a few tenths of a percent can be determined.

A time series of these measurements, with a prelaunch functional form of $e^{-\beta t}$, gives the relative change in instrument responsivity over the MODIS mission lifetime. Here t is the time after start of on-orbit operations and β is the slope of the fitted curve. This functional form allows the interpolation of the responsivity between solar measurements. Once an understanding of the long-term responsivity changes in the instrument are understood, it may be possible to use functional form to predict responsivity changes. Again, the emphasis centers on understanding. The responsivity correction will not be applied automatically. It will wait for an understanding of the instrument characteristics on orbit. The prelaunch functional form presented here may also be replaced.

By combining these three parts, the on-orbit radiance responsivity is given by

$$L^* = \delta_{cal} \delta_{tto} e^{\beta \cdot t} \quad (4)$$

3.1.1.1 Effective Digital Counts

There are corrections to the MODIS digital counts that MCST understands how to make; this understanding comes from analysis of EM data. Additional corrections are expected after PFM testing, analyses, and interpretation.

In the reflected solar bands, the radiometric and reflectance calibration algorithm corrects for systematic effects due to focal plane temperature, mirror side, scan angle, and quantization errors of the A/D converters. These corrections will apply to all radiance sources, including the radiance from the SRCA, SD, and EV. When in lunar mode (the moon is visible the SV port), the SV will also be a source of radiance and will have the complete set of corrections applied. When not in lunar mode, the SV data are corrected for quantization errors only. The following corrections are applied to each reflected solar band and detector for each scan line:

(1) Correct digital numbers for A/D nonlinearity effects.

There are a total of fourteen A/D converters used to generate the digital numbers (DN) from the MODIS focal planes. Twelve of these (6 per mirror side) are used for the reflected solar band focal planes. Ground tests will measure deviations from linearity for each A/D converter, and most of the MODIS reflected solar band DN values will be corrected for quantization effects with a table lookup of the form $Q(AD_B, DN_{B,D})$ where B =Band, and D =Detector. Instrument limitations in the bands that use Time Delay Integration (TDI) prohibit the quantization correction for bands 13 low, 13 high, 14 low, or 14 high. For these bands both $Q(AD_{13}, DN_{13,D})$ and $Q(AD_{14}, DN_{14,D})$ are equal to DN. The A/D correction will vary from zero to about 6 DN over the 4096 DN range of the converters. The residual uncertainty from this correction is estimated to be about 2 DN.

(2) Filter and average zero radiance offset and correct measured DN.

For scan lines where the moon is not present in the SV port, the corrected SV data are averaged and filtered to produce the SV count buffer average, $\langle Q(AD_B, DN_{0B,D}) \rangle$. This is the zero radiance offset. The SV count buffer average is then subtracted from the corrected radiance DN. The same correction is applied to SD, EV, SRCA, and lunar data (SV data when the moon is visible in the SV port).

(3) Correct measured DN for focal plane temperature effects

A linear correction is applied for the difference between a reference temperature, $T_{REF}(FP_B)$, of a focal plane and the average focal plane temperature, $\langle T(FP_B) \rangle$, where FP_B is the focal plane for band B. The temperature coefficient, $K_{B,D}$, is determined for each MODIS detector, with the determination based on responsivity variations observed during thermal vacuum testing. The magnitude of the temperature coefficient should range from about 0.01% to about 0.1% per degree. Within an orbit, the temperature of the uncooled reflected solar focal plane is expected to change by about one to two degrees. The uncertainty in the short-term temperature correction is expected to be negligible. Over the life of the mission, MODIS will warm by ten or more degrees as the thermal blankets lose efficiency. For the reflected solar bands, any deficiency in this correction will become part of the long-term responsivity change.

(4) Correct measured DN for scan angle effects

The mirror reflectance depends on the angle at which the mirror is viewed. The reference for this is the normal to the scan mirror surface. The correction is applied through a lookup table $S(B,D,MS,F_{eqv})$ that includes differences in the reflectances of the two sides of the scan mirror, where MS=mirror side. The lunar, SRCA, and SD data segments are mapped into an equivalent Earth View frame number, F_{eqv} , based on their incidence angles relative to the normal to the scan mirror surface. Side-to-side differences in the scan mirror reflectivity will be substantially less than 1%, particularly near nadir. For the reflected solar bands, the reflectivity of the mirror can change by up to 5%, relative to nadir, for measurements near the edge of the swath.

After these corrections for instrument effects have been applied, the notation for the uncorrected digital counts (the DN^* in the basic equation) is changed to DN^* , known as effective digital counts. These counts are, in effect, those that the instrument would be expected to produce under laboratory conditions. DN^* is part of the process of carrying the laboratory calibration to the scene that MODIS views on orbit.

The complete correction from DN to effective DN, DN^* , is

$$DN^*_{B,D} = \left[Q(AD_B, DN_{B,D}) - \langle Q(AD_B, DN_{0_{B,D}}) \rangle \right] \cdot \left[1 + K_{B,D} (\langle T(FP_B) \rangle - T_{ref}(FP_B)) \right] \cdot [S(B, D, MS, F_{eqv})] \quad (5)$$

The SD/SDSM algorithm (see Sections 3.1.1.2 and 3.1.1.3) yields the responsivity which, in turn, yields the equation for the Earth view radiance from MODIS detector counts

$$L_{EV,B,D} = \frac{DN_{EV,B,D}}{F_{VC,L,B} \quad L_{B,D}} \quad (6)$$

The equation for the product of the Earth view bi-directional reflectance and the Earth view solar zenith angle from MODIS detector counts is given by

$$[\rho_{ev} \cos(\theta_{ev})]_{B,D} = \frac{DN_{ev,B,D}}{F_{VC,\rho,D} \quad \rho_{B,D}} \quad (7)$$

B - Band

D	- Detector
$DN_{ev,B,D}$	- Effective detector counts at the Earth scene
$F_{VC,L,B}$	- Radiance calibration correction factor from vicarious data
$F_{VC, ,}$	- Reflectance calibration correction factor from vicarious data
$^*_{L,B,D}$	- Radiance responsivity
$^*_{,B,D}$	- Reflectance responsivity
θ_{ev}	- Solar zenith angle at Earth scene
ρ_{ev}	- Scene bidirectional reflectance factor

Equations (6) and (7) are applied to each pixel in each scene to convert the outputs from MODIS into L1B data products. The effective digital counts and responsivities in these equations are generated from internal MODIS measurements. The correction factors are a means of incorporating the results of vicarious measurements into the equations. The incorporation of these corrections will derive from the judgment of a panel of experts. The radiance responsivity term is discussed in Section 3.1.1.2, the reflectance responsivity in Section 3.1.1.4, and vicarious calibration in Section 3.4.

3.1.1.2 Radiance Responsivity

The solar calibration period lasts approximately two minutes during which time SD scan averages and SDSM sample averages are computed. The following notation and equations define the reflected solar band calibration.

S	Scan mirror counter
$BRDF_0$	Prelaunch-measured SD BRDF in band B, scan S $[sr^{-1}]$
$DN_{SD,B,D,S}$	Average effective count for one scan of the SD
$DN_{ev,B,D}$	Effective count for one pixel of the Earth View
$N_{SD,B,D}$	Number of scans of the SD during the solar calibration period
$E_{sun,B}$	At-aperture solar spectral infrared radiance in band B $[W m^{-2} \mu m^{-1}]$ adjusted for Earth-Sun distance
$^*_{L,B,D}$	Radiance responsivity estimated from SD $[counts W^{-1} m^2 sr \mu m]$
$^*_{,B,D}$	Reflectance responsivity estimated from SD $[counts]$
$L_{ev,B,D}$	Earth View spectral radiance $[W m^{-2} sr^{-1} \mu m^{-1}]$
$L_{SD,B,D}$	SD spectral radiance $[W m^{-2} sr^{-1} \mu m^{-1}]$
θ_{SD}	Solar zenith angle relative to the SD normal
$T_{SD,S}$	Transmittance of the SD screen (nominal 8.5%)
b	SDSM band number (1-9)
s	SDSM sample number (1-20)
$C_{SD,b,s}$	SDSM average count value for one SD sample (3 points/sample)
$C_{sun,b,s}$	SDSM average count value for one solar sample
$BRDF_{b,s}$	SDSM estimate of SD BRDF in band b, sample s $[sr^{-1}]$
$BRDF_{A\&E,b,s}$	SDSM estimate of SD BRDF in A&E for band b, sample s $[sr^{-1}]$
θ_{SDSM}	Solar zenith angle relative to the SDSM screen normal

τ_{SDSM}	Transmittance of the SDSM screen (nominal 2%)
$K_{SD,b}$	SDSM responsivity for SD sampling in SDSM band b
$K_{sun,b}$	SDSM responsivity for solar sampling in SDSM band b
$N_{SDSM,b}$	Number of SDSM samples during the solar calibration period
B	SD degradation factor in SDSM band B

During a solar calibration period, each MODIS mirror side scans the SD approximately 81 times, collecting up to 15 usable samples per scan for each detector in a band for 1 km IFOV (30 samples for 0.5 km IFOV, and 60 samples for 0.25 km IFOV). During each mirror scan 15 samples of the SV are also collected. All of the sample DN's within a scan are converted into effective DN's using the correction terms in equation (4) from section 3.1.1.1. The resulting DN's are filtered for outliers and averaged. For each of these averages, the radiance from the solar diffuser is calculated using equation (8). Since the detector responses are highly linear with respect to input infrared radiance, the resulting set of effective SD scan averages for each detector in the 20 solar reflective bands are linearly regressed on the SD radiances using a straight-line model with zero-intercept. From the linear fit of DN versus SD radiance for each detector's responsivity is estimated from the slope of the linear fit.

$$L_{B,D} = \frac{\sum_{S=1}^{N_{SD,B,D}} L_{SD,B,S} DN_{SD,B,D,S}}{\sum_{S=1}^{N_{SD,B,D}} L_{SD,B,S}^2} \quad (8)$$

where

$$L_{SD,B,S} = E_{sun,B} \tau_{SD,S} B BRDF_{0,B,S} \cos(\theta_{SD})_S, \quad (9)$$

and where $\tau_{SD,S}$, and $BRDF_{0,B,S}$ are read from lookup tables, and $E_{sun,B}$, is the solar infrared radiance, adjusted for the Earth-Sun distance, and B is the SD degradation factor in SDSM band B. The purpose for the SDSM on MODIS is the determination of B .

The radiance in Equation (9) is a reference value, calculated for each solar calibration. For the MODIS radiance responsivities, this radiance need not be known on an absolute scale. Equations (8) and (9) are used solely to monitor long-term changes, on a relative basis, in the responsivities. The solar infrared radiances in Equation (9) come from the Wehrli (1985) compilation and are weighted by the relative spectral responses of the bands. In addition, these band-averaged infrared radiances are corrected in $E_{sun,B}$ for changes from the nominal 1 AU Earth-Sun distance in the Wehrli (1985) compilation. The use of equations (8) and (9) requires the assumption that the solar infrared radiance does not change, not that it is known exactly.

The responsivities, $L_{B,D}$, are then appended to the response-history file, and regressed with time using the exponential model prediction $L_{B,D}^* = \exp(\beta_{B,D}^0 + \beta_{B,D}^1 t)$, where t is the time of the solar calibration period, and $\beta_{B,D}^0$ and $\beta_{B,D}^1$ are the slope and intercept, respectively, of the responsivity prediction function for each detector in band B. The responsivity prediction function is updated with each solar calibration in the L1B operational processing to calculate values of the instrument

responsivities $\tau_{L,B,D}^*$. Uncertainties in the predicted responsivities are based on prediction intervals computed using standard linear regression techniques [Seber, 1977]. In addition the prediction bands serve as lower and upper bounds for detecting anomalous responsivities resulting from solar calibration processing.

At the start of on-orbit operations, that is, at a time very close to zero in the responsivity prediction function, the radiance scales of the reflected solar bands will be transferred to the solar diffuser (Veiga et al. 1996). Mathematically, this scale transfer will define β_0 and force agreement between the responsivity prediction function and Equation (4) at $t=0$.

3.1.1.3 Calculation of β_B

The SDSM functions to monitor the degradation of the SD on orbit. This information is fundamental to the determination of long-term changes in the radiance responsivities. The term β_B allows the separation of changes in the solar diffuser from changes in MODIS.

Throughout a solar calibration period, as the MODIS scan-mirror sweeps across the SD, the SDSM independently samples the SD and Sun. Care must be taken to ensure that the SDSM samples are synchronized with the SD samples. The mapping of offset-corrected SDSM counts from SD sampling to SD infrared radiance is given by

$$C_{SD,b,s} = E_{sun,b} \tau_{SD,s} \cos(\theta_{SD})_s BRDF_{b,s} K_{SD,b}, \quad (10)$$

where $C_{SD,b,s}$ gives the offset corrected counts from the SDSM measurement of the ratio. A nominal value for the solar irradiance is sufficient for the calculations in this section, since the irradiance will be eliminated in Equation (12).

Simultaneously, SDSM counts from Sun sampling are converted to solar infrared radiance by

$$C_{sun,b,s} = E_{sun,b} \tau_{SDSM} \cos(\theta_{SDSM})_s K_{sun,b} \quad (11)$$

where the SDSM responsivities $K_{SD,b}$, and $K_{sun,b}$ are the SDSM responsivities for SD sampling and Sun sampling, respectively. The ratio $K_{sun,b}/K_{SD,b}$ is assumed to be constant throughout the mission life. This assumption is central to the use of the SDSM as a ratioing radiometer, and it will be checked on orbit. The estimate of the SD BRDF from SDSM samples is calculated from the ratio of equations (11) and (12) as

$$BRDF_{b,s} = \frac{C_{SD,b,s} \tau_{SDSM} \cos(\theta_{SDSM})_s K_{sun,b}}{C_{sun,b,s} \tau_{SD,s} \cos(\theta_{SD})_s K_{SD,b}} \quad (12)$$

The screen transmittances are read from lookup tables, and each SDSM sample corresponds to the current solar incidence geometry. To compute the degradation of the SD, the current BRDF factor,

$BRDF_{b,s}$, is ratioed with the BRDF factor, $BRDF_{A\&E,b,s}$, measured by the SDSM during A&E. The initial BRDF factors from A&E are calculated in the same manner as equation (11)

The SD degradation factor, b , at the nine SDSM wavelengths is defined as

$$b = \frac{1}{N_{SDSM,b}} \frac{\sum_{s=1}^{N_{SDSM,b}} BRDF_{b,s}}{BRDF_{A\&E,b,s}} \quad (13)$$

Using the measured b , linear interpolation over wavelength is used to obtain the SD degradation, b_B , in the MODIS band B. The SD degradation factor, b_B , is applied in equation (12) and, is part of the regression that determines $K_{L,B,D}$ in equation (11). For the MODIS bands with band-center-wavelengths longer than any of the SDSM measurements, the longest wavelength value of b_B will be used. Since the SDSM receives back-scattered radiance from the SD, the assumption is made that b_B applies to the forward scattering direction, the direction of the MODIS scan mirror.

3.1.1.4 Reflectance Responsivity

In addition to its function as a radiometer, MODIS will be used on orbit as a reflectometer. In this mode, MODIS will act as a transfer radiometer between two diffuse reflecting surfaces, the solar diffuser and the Earth. MODIS uses the solar diffuser as a reference sample. The preflight laboratory characterization of the diffuser determines its reflectance properties, that is, its radiance to irradiance reflectance ratio, using a standard diffuser from NIST. Here, the ratio is called the solar diffuser bidirectional reflectance factor, ρ_{sd} , with units of sr^{-1} .

On-orbit, both the SD and the Earth will be illuminated by the same irradiance source. For the MODIS solar diffuser, the reflectance is given by

$$\rho_{sd} = \frac{L_{sd}}{E_i \cos(\theta_{sd})} \quad (14)$$

where

L_{sd} = Spectral radiance from the diffuser measurement

ρ_{sd} = Bidirectional reflectance factor

E_i = Solar irradiance (a nominal constant for this value is sufficient, since the irradiance will be eliminated from the calculation in Equation (16))

θ_{sd} = Irradiance incidence angle

The term $\cos(\theta_{sd})$ accounts for the geometric expansion of the irradiance beam for angles other than normal incidence to the diffuser surface. In this presentation, the use of the coefficients for the elevation and azimuth angles for incidence and reflectance is minimized to simplify the equations. In addition, the geometric factor for the Earth-Sun distance in the solar diffuser and Earth view measurements is not shown here. This factor accounts for non-contemporaneous solar

diffuser and Earth view measurements which, late in the mission, may be up to a week or more apart. This factor is part of the L1B algorithm and need not be applied by the user.

When viewing the earth the reflectance is given by,

$$\rho_{ev} = \frac{L_{ev}}{E_i \cos(\theta_{ev})} \quad (15)$$

Equations (14) and (15) can be combined to give

$$\rho_{ev} \cos(\theta_{ev}) = \frac{L_{ev}}{L_{sd}} \rho_{sd} \cos(\theta_{sd}) \quad (16)$$

Equation (16) shows the use of MODIS as a ratioing radiometer with the solar diffuser as a reference sample. Using Equation (6) and (6) with ev changed to sd, it is possible to convert the SD and Earth-view radiances into effective digital counts.

$$[\rho_{ev} \cos(\theta_{ev})]_{B,D} = \frac{DN_{ev,B,D}}{DN_{sd,B,D} / \rho_{sd,B} \cos(\theta_{sd})} \quad (17)$$

The reflectance responsivity is defined as

$$\rho_{ev,B,D} = \frac{DN_{ev,B,D}}{\rho_{sd,B} \cos(\theta_{sd})} \quad (18)$$

and

$$\rho_{sd,B} = \frac{DN_{sd,B,D}}{\rho_{cal,sd,B}} \quad (19)$$

For reflectance measurements, $\rho_{cal,sd,B}$ is the initial laboratory reflectance calibration of the bidirectional reflectance function of the diffuser plate. It is the reflectance analog of the preflight radiance calibration of MODIS. However, unlike the radiance calibration, there is no method to monitor changes in this calibration from the laboratory to orbit. There is no analog to the ρ_{TTO} term in equation (4). The long-term change in the bidirectional reflectance factor of the solar diffuser is calculated from SDSM measurements using $\rho_{sd,B}$, as shown in Section 3.1.1

3.1.1.5 Uncertainty Estimate

The fractional uncertainty in the MODIS calculated reflectance (ρ_{ev}) has several components. There include the uncertainty in the algorithm, in the laboratory calibration of the BRDF characteristics of the diffuser, and in the effects of polarization, crosstalk, and scatter within the instrument. These last three components will be scene dependent, and their magnitude is currently not known.

$$\frac{\rho_c}{\rho_c} = \sqrt{\frac{\rho_c}{\rho_c}_{\text{algorithm based}}^2 + \frac{BRDF}{BRDF}_{\text{solar-diffuser}}^2 + \frac{\rho_c}{\rho_c}_{\text{polarization}}^2 + \frac{\rho_c}{\rho_c}_{\text{crosstalk}}^2 + \frac{\rho_c}{\rho_c}_{\text{scatter}}^2} \quad (20)$$

Within the algorithm there are short-term uncertainties in the calculation of effective digital counts, uncertainties in the long-term determination of the responsivity and in the annual change in the Earth-Sun distance.

$$\frac{\rho_c}{\rho_c}_{\text{algorithm-based}} = \sqrt{\frac{DN}{DN}^2 + \frac{\rho}{\rho}^2 + \frac{R_l}{R_l}_{\text{Relative Earth-sun Distance Factor}}^2} \quad (21)$$

The uncertainties in the effective digital counts include those in the terms that make up Equation (5). The uncertainty in the sample timing correction for the 250- and 500- meter reflected solar bands is also included here.

$$\frac{DN}{DN} = \sqrt{\frac{Q}{Q}_{\text{ADC}}^2 + \frac{Fr}{Fr}_{\text{Sample Timing Correction}}^2 + \frac{K}{K}_{\text{FPA Temperature Coefficient}}^2 + \frac{T}{T}_{\text{FPA Temperature}}^2 + \frac{R}{R}_{\text{mirror-side correction}}^2 + \frac{R(\)}{R(\)}_{\text{scan angle}}^2} \quad (22)$$

The algorithm portion of the uncertainty in the reflectance responsivity is dominated by the uncertainty in the slope of the responsivity prediction function ().

$$\frac{\rho}{\rho} = \sqrt{\frac{\beta}{\beta}^2 + \frac{\tau_{SD}}{\tau_{SD}}^2} \quad (23)$$

The same method can be used to combine the individual radiance uncertainties into an RSS sum.

The following table shows the current uncertainty estimates for four MODIS reflected solar bands. They include the shortest wavelength (0.41 μm) and the longest wavelength (2.13 μm) bands. The two shorter wavelength bands have 1000 m IFOVs; the two others are 500 m bands. The 500 m bands have an possible sample timing error that is an artifacts of the instrument's subsampling technique. This adds an uncertainty to the table that is not found in the 1000 m bands.

Table 3.1.1 shows the major contributors to the error budget to the laboratory calibration of the bands, the sample timing errors in the 500 m bands, and the signal noise (the reciprocal of the signal-to-noise ratio) in the 1.24 μm band. The algorithm dependent terms, as given in Equations (5), (6), and (7), are minor contributors to the error budget.

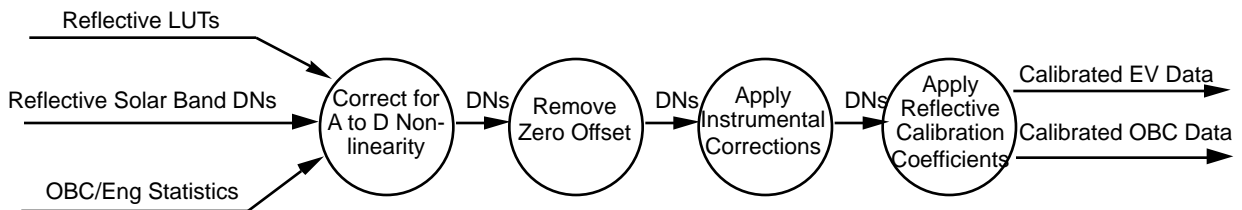
TABLE 3.1.1 Radiance & Reflectance Calibration Uncertainties

Radiance Calibration Uncertainties (%)				
	Band 8	Band 15	Band 5	Band 7
Uncertainty Source	(0.41 μm)	(0.75 μm)	(1.24 μm)	(2.13 μm)
NIST to SIS100 Transfer (per GSFC experience)	2.3	1.3	1.5	2.4
Transfer to MODIS	1.0	1.0	1.0	1.0
Signal Noise (1/SNR at L _{typical})	0.1	0.2	1.4	0.9
ADC Quantization Correction	0.2	0.1	0.6	0.7
Sample Timing Errors (Estimated)	0.0	0.0	1.0	1.0
FPA Temperature Correction	0.1	0.1	0.3	0.4
Scan Angle Reflectance Correction	0.2	0.1	0.5	0.5
Mirror Side Correction	0.2	0.1	0.7	0.7
Polarization (Scene Dependent)	---	---	---	---
Crosstalk (Scene Dependent)	---	---	---	---
Scatter (Scene Dependent)	---	---	---	---
RSS Total	2.5	1.6	2.7	3.2
Reflectance Calibration Uncertainties (%)				
	Band 8	Band 15	Band 5	Band 7
Uncertainty Source	(0.41 μm)	(0.74 μm)	(1.24 μm)	(2.13 μm)
SD BRDF Variation and Measurement	2.0	2.0	2.0	2.0
SD Degradation Not Monitored by SDSM	0.5	0.5	0.5	0.5
SD Screen Transmittance	0.5	0.5	0.5	0.5
SD Port Scatter	0.1	0.1	0.1	0.1
Signal Noise (1/SNR at L _{typical})	0.1	0.2	1.4	0.9
ADC Quantization Correction	0.2	0.1	0.6	0.7
Sample Timing Errors (Estimated)	0.0	0.0	1.0	1.0
FPA Temperature Correction	0.1	0.1	0.3	0.4
Scan Angle Reflectance Correction	0.2	0.1	0.5	0.5
Mirror Side Correction	0.2	0.1	0.7	0.7
Polarization (Scene Dependent)	---	---	---	---
Crosstalk (Scene Dependent)	---	---	---	---
Scatter (Scene Dependent)	---	---	---	---
RSS Total	2.2	2.1	2.9	2.8

3.1.2 Product Flow in the Algorithm

The prediction bands on the linear responsivity trend functions will be assessed in the CROM for their validity in estimating radiance and reflectance uncertainties.

The L1B reflective band calibration data flow diagram is :



3.1.2.1 Programming Considerations

The software implementation of the algorithm takes into consideration efficient use of computing resources and ease of maintenance in the production environment. The software system makes extensive use of look-up tables instead of direct computations. Look-up tables are generated in the CROM. This technique reduces CPU requirements in the production environment by moving computation of stable or slowly varying terms out of the time-critical production stream. Changes to instrument characteristics or to the way these characteristics are determined are provided as updated input datasets rather than new versions or releases of the production software. These tables are sized to include expected parameter ranges with a resolution determined to minimize both interpolation errors and software memory use.

3.1.2.2 Quality Control and Diagnostics

Outlier detection is included in the algorithm to filter the populations of the SV, SD, and SDSM count data. The algorithm for the SV never considers more than a small fraction of the SV data as outliers, so that a minimum sample size will always be available from the space port. Outliers in the SD and SDSM count data are filtered since these data are critical to accurate calibration.

SD quality assurance is maintained by comparison of the irradiances computed from degradation-corrected SD measurements with a so model integrated over the bandpasses of the corresponding MODIS bands [Kurucz, 1984]. Significant deviations in the comparison indicates that problems may have occurred in SD BRDF estimation.

For the 11 bands which can be calibrated with both SD modes (screen-up and screen-down), time series of the responsivity ratios derived from each SD mode will be monitored for information on SD screen transmittance changes.

SDSM detector health is monitored using the BRDF calculations in equation 11 and by assuming smooth changes in the reflectivity of the SD over periods of weeks to months. A detector's count data will be excluded from the SD degradation estimation if there is significant deviation by a detector from the established trend. The SD degradation interpolation algorithm that determines τ_B from τ_b (see Section 3.1.1.2) will be modified accordingly. The historical record of goodness of fit of the SD count data to a straight line (with intercept) will be monitored, and thereby provide an estimate of detector stability in the range of SD radiances experienced during solar calibration periods.

3.1.2.3 Exception Handling

The following events are flagged in the output data: Moon in the SV Port, Spacecraft Maneuver, Sector Rotation, Negative Radiance Beyond Noise Level, PC Ecal On, PV Ecal ON, SD Door Open, SD Screen Down, SRCA On, SDSM On, Outgassing, Instrument Standby Mode, Linear Emissive Calibration, DC Restore Change, BB/Cavity Temperature Differential, BB Heater On,

Missing Previous Granule, Missing Subsequent Granule, Missing from Level 1A Dataset, Dead Detector, Saturated Value, Calibration Failure, Radiance Too Low to Calculate, Coherent SV Noise, Number of SV Outliers Exceeded Maximum, Mirror Side Difference in SV Data. Messages describing these exceptions are written to the message logs using the Status Messaging Facility (SMF) supported in the Science Data Processing Tool Kit (SDPTK).

3.1.2.4 Output Product

For each of the 330 detectors in the solar reflective bands 1-19, and 26 the L1B calibration product consists of the Earth scene spectral radiance, product of the Earth scene BRF with cosine of the scene zenith angle, along with their associated uncertainties (radiance and reflectance uncertainties are composed of the current best bias component combined in RSS with the sample random component). These products are derived by analysis of SV output that consists of seven statistics characterizing the SV, as well as SV radiance, BRF, and their associated uncertainties. In addition SD output data are generated after each solar calibration period. They include SD effective counts, estimated radiance responsivities, BRF calibration coefficients, responsivity trend parameters (intercept and slope), BRF calibration coefficient trend parameters, and scan-mirror-side relative reflectances. See Appendix F for a description of L1B output products.

3.2 The Emissive Infrared Bands

3.2.1 Basic Measurement Equation

The MODIS emissive infrared band response is expected to be predominately linear, therefore, the baseline equation retrieving the band-averaged Earth view radiance, L_{ev} , is derived through the following basic linear equation relating the detector voltage response to the incoming radiance as

$$V_s = m \left(\rho_{s,\lambda} L_{s,\lambda} R_{\lambda}^{opt} d\lambda + (1 - \rho_{s,\lambda}) B_{mir,\lambda} R_{\lambda}^{opt} d\lambda + L_{bkg} \right) + V_0 \quad (24)$$

where

- s an index, indicating emissive sources of bb, sv, ev.
- V_s Analog signal voltage from Focal Plane (FPA) when the scan mirror is viewing bb, sv, ev.
- m Linear calibration coefficient or system gain.
- V_0 Zero flux output voltage from the detector.
- $\rho_{s,\lambda}$ On-orbit scan mirror spectral reflectivity.
- $L_{s,\lambda}$ Spectral radiance coming to the scan mirror when the scan mirror is viewing the source s .
- R_{λ}^{opt} Optical Relative Spectral Response (RSR), which, after being multiplied by the scan mirror reflectivity $\rho_{s,\lambda}$, gives the system RSR, R (which is a function of scan mirror angle).
- $B_{mir,\lambda}$ Planck spectral radiance evaluated at the scan mirror temperature, and the associated term $(1 - \rho_{s,\lambda}) B_{mir,\lambda}$ is accounted for the scan mirror thermal emission.
- L_{bkg} Optical background radiance.

After some re-arrangement of the terms in Eq.24, the basic linear equation becomes

$$V_s = m L_s + V_0, \quad (25)$$

where

$$L_s = D_s \int_0^s \rho_{s,\lambda}^g (L_{s,\lambda} - B_{mir,\lambda}) R_\lambda^{opt} d\lambda, \quad (26)$$

the offset $V_0 = V_0 + mL_0$, and $L_0 = \int_0^s B_{mir,\lambda} R_\lambda^{opt} d\lambda + L_{bkg}$.

The scan mirror reflectivity $\rho_{s,\lambda}$ is replaced by $D_s \rho_{s,\lambda}^g$, where $\rho_{s,\lambda}^g$ is the prelaunch measured scan mirror reflectivity, and D_s is the corresponding correction factor determined on-orbit by viewing the cold space through the Earth aperture during a spacecraft maneuver. However, what is measured during a spacecraft maneuver is the system RSR rather than the scan mirror reflectivity; consequently D_s can be defined as the system level Response vs Scan Angle (RVS) correction. Since only one side of the scan mirror reflectivity is measured prelaunch, the on-orbit correction term, D_s , will be mirror side dependent.

Applying Eq.25 to the OBC blackbody and space view measurements, the two calibration parameters, m and V_0 , can be determined as

$$m = \frac{V_{bb} - V_{sv}}{L_{bb} - L_{sv}}, \quad (27)$$

$$V_0 = \frac{V_{sv} L_{bb} - V_{bb} L_{sv}}{L_{bb} - L_{sv}}, \quad (28)$$

and the basic measurement equation for the L1B band-averaged radiance product is

$$L_{ev} = B_{mir} + \frac{V_{ev} - V_0}{m} R_\lambda d\lambda, \quad (29)$$

which is applied on a per pixel basis. The band-averaged radiance L_{ev} is traditionally defined as

$$L_{ev} = \frac{\int_0^s L_{ev,\lambda} R_\lambda d\lambda}{\int_0^s R_\lambda d\lambda}, \quad (30)$$

and so is the band-averaged Planck radiance B_{mir} evaluated at scan mirror temperature. Note that Eq.29 relates the Earth view radiance to the FPA voltage, and the basic equation relating voltage to the raw Digital Number (DN) will be discussed in section 3.2.2.4.

3.2.1.1 The Master Curve Premise and Quadratic Calibration Equation

The MODIS emissive infrared band response is expected to be predominately linear. More generally it can be described as a quadratic function of the detector total incident radiant flux [T. Pagano, 1993; I.L.Goldberg, 1995] as

$$V_s = a(s + P_x)^2 + b(s + P_x) \quad (31)$$

where s represents the radiant flux incident on the detector, a and b are calibration coefficients, and P_x represents the instrument background flux and bias. This is the MODIS calibration master curve proposed by SBRS applicable to both the PV and PC detector bands. For MODIS the DC restore voltage corresponding to P_x is continuously available from the telemetry, therefore, Eq.31 can be directly applied. This varies from the traditional formulation used for some heritage instruments where the derived flux (or radiance) is a quadratic function of the output voltage and the functionality involves a differential signal instead of the absolute signal.

The MODIS instrument incorporates hardware and on-board software features to continuously apply a DC restore voltage to the PV and PC preamplifiers so as to maintain the dynamic range within the specified limits as the instrument background changes as a result of instrument temperature changes (N.B., the FPA temperatures are considered separately). As the background flux changes the calibration curve (equation) characterizing the instrument response is considered to be constant. This is shown in Figure 3, where the location of the dynamic range along the master curve shifts due to the P_x , but the calibration curve stays constant.

The calibration curve will vary as the FPA temperature changes. However, the MODIS has been designed to maintain a "closed loop" temperature control of the SWIR/MWIR and LWIR FPAs within narrow temperature control limits ($83 \pm 0.005\text{K}$, $85 \pm 0.005\text{K}$ and $88 \pm 0.005\text{K}$). Thus, only a few (three as planned) FPA temperature conditions need to be tested prelaunch to characterize the calibration curve as a function of the FPA temperature. In addition to this closed loop mode, both of the focal planes, located on the common cold stem of the radiation cooler, can be operated "open loop" by commanding the temperature control heaters off. This feature is accommodated by setting an additional testing point at 79K.

Clearly, to the extent that the master curve equation is a valid representation of the instrument response, a significant reduction in thermal vacuum testing can be realized since the same calibration equation should apply to a wide range of instrument temperatures.

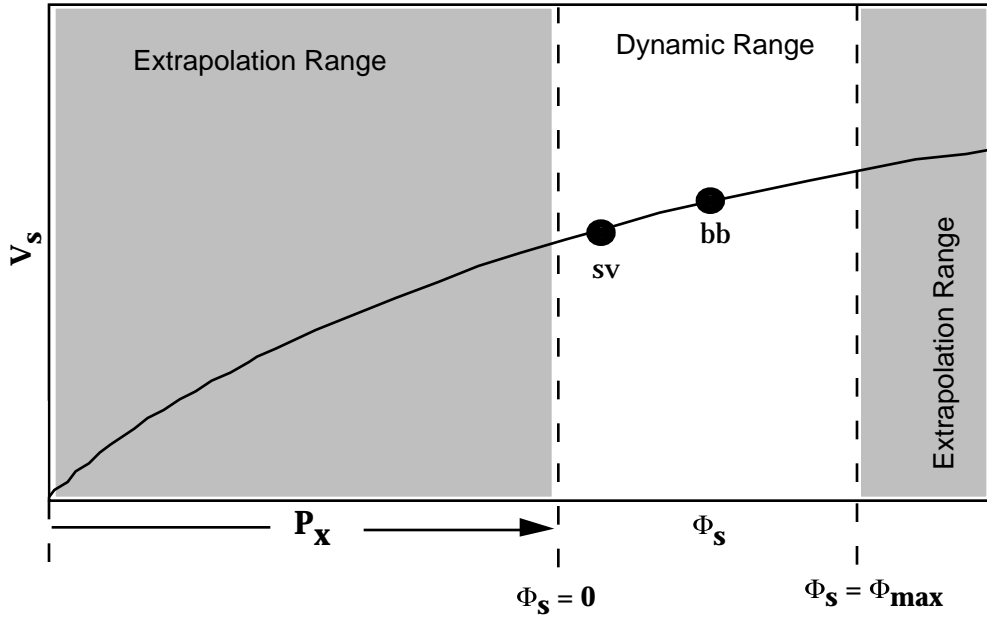


Figure 3. The emissive band calibration master curve .

Based on the master curve Eq.31, the following system level at-aperture radiance equation can be derived [Knowles, 1996],

$$V_s = \alpha m^2 (L_s + L_0)^2 + m(L_s + L_0) \quad (32)$$

where

α Pre-launch measured system nonlinearity ($\alpha = a/b^2$ with respect to Eq.31).

m Linear calibration coefficient or system gain.

L_s As defined in Eq.26.

L_0 Background radiance and bias.

Note that as the system nonlinearity α goes to zero, Eq.32 becomes identical to the linear equation of Eq.25, except that V_0 in Eq.24 has been absorbed in L_0 . There are three calibration parameters, α , m and L_0 , captured in Eq.32. The non-linearity α will be measured prelaunch at four FPA temperature conditions mentioned above, and will be interpolated on-orbit based on the FPA temperature. The other two parameters will be determined every scan by using the BB and SV measurements as

$$m = \frac{\sqrt{1 + 4\alpha V_{bb}} - \sqrt{1 + 4\alpha V_{sv}}}{2\alpha(L_{bb} - L_{sv})}, \quad (33)$$

$$L_0 = \frac{-1 + \sqrt{1 + 4\alpha V_{sv}}}{2\alpha m} - L_{sv} \quad (34)$$

and probably, pending analysis of PFM thermal vacuum testing data, a few scans will be used to obtain an averaged and therefore relatively constant m and L_0 over many scans.

The final L1B band-averaged Earth scene radiance product is

$$L_{ev} = B_{mir} + \frac{-1 + \sqrt{1 + 4\alpha V_{ev}} - 2\alpha m L_0}{2\alpha m R_\lambda d\lambda}, \quad (35)$$

which is applied on a per pixel basis. Indices describing the appropriate level of detail (pixel, frame, scan number and mirror sides) are suppressed at this summary level. They are described in specific detail in Section 3.2.2.4. Note that as α goes to zero, Eqs. 33-35 collapse to the corresponding linear equations 27-29, which becomes evident by observing the expansion of the square root to the first order of α , $\sqrt{1 + 4\alpha x} \approx 1 + 2\alpha x$, and linear equation offset $V_0 = mL_0$.

The linear calibration equations will be used as the Level 1B emissive infrared band baseline calibration equations, and the quadratic ones will be used only when the prelaunch thermal vacuum test data shows a non-zero α and a significant improvement of quadratic fitting versus linear fitting.

3.2.1.2 Conversion from MODIS Counts to Detector Preamplifier Output Voltage

The analog detector preamplifier voltage output is converted to digital counts by an Analog to Digital Converter (ADC). Each of the ADCs is mapped by determining the digital output (12 bit) in response to precisely controlled voltage increments from a 16 bit voltage supply source. This mapping will be represented as prelaunch LUTs. Also, the ADC nonlinearity effects will be measured and incorporated in prelaunch LUTs. A combined LUT representing these results is $V_{ADC}\{DN\}$, denoting the input voltage to an ADC with the given output DN.

For the PV bands, the digital counts to voltage transfer equation is

$$V_s^{PV} = \frac{V_{ADC}\{DN_s\}}{G_1 G_2 G_3 G_4} - V_{DC}^{PV}, \quad (36)$$

where four gain factors and one DC restore voltage value (continuously adjusted by an on-board software algorithm and reported by telemetry) are applied. G_1 , G_2 and G_4 are fixed hardware values, and G_3 can be changed by command uploads to periodically restore the output dynamic range to specified values.

For the PC bands, the digital counts to voltage transfer equation is

$$V_s^{PC} = \frac{V_{A/D}\{DN_s\}}{G_1 G_2} - V_{DC}^{PC}, \quad (37)$$

where

$$V_{DC}^{PC} = \frac{V_{DC2}}{G_1} + V_{DC1}, \text{ and two fixed gain factors and two adjusted DC restore voltages are applied.}$$

It should be noted that for the basic linear calibration equation, the L1B radiance of Eq.29 does not depend on the gain and DC restore values, since they are all canceled out in L_{ev} calculation.

3.2.1.3 The Calibration Transfer

MODIS uses an aluminum v-groove blackbody mounted inside the scan cavity as its emissive infrared band on-board calibrator. The radiometric calibration transfer to the BB is accomplished by determining the effective BB emissivity and temperature using the prelaunch BCS standard and vicarious calibration. The basic calibration transfer equation can be expressed as

$$\min_{T_{bb}, \epsilon_{bb}} \left| L_{bcs} - L_{bcs}^{L1B} \left\{ L_{bb} (\epsilon_{bb} + \epsilon_{bb} T_{bb} + T_{bb}) \right\} \right|, \quad (38)$$

where L_{bcs} is the input BCS standard radiance, and L_{bcs}^{L1B} is the L1B output BCS radiance calculated by using the BB and SV measurements, shown in Eq.29 or 35. The ϵ_{bb} is the blackbody nominal emissivity measured (or modeled) in the laboratory, and T_{bb} is the blackbody thermistor reading of the blackbody temperature. Equation 38 is the process of tuning the offset ϵ_{bb} and T_{bb} to minimize the difference of the input and output BCS radiance. This process will be done for each emissive infrared band at prelaunch using thermal vacuum test data; ϵ_{bb} and T_{bb} will be represented as LUTs.

After launch, vicarious calibration will provide the opportunity of the postlaunch calibration transfer to the BB, where the same minimizing process of Eq.35 will be applied to the known ground sources calibrated with other instruments.

3.2.1.4 Summary of the Calibration Parameters

For the purpose of simplicity, the detail levels of indices are suppressed when the top level of the calibration equations were presented in the previous sections. In this section, a summary of the calibration parameters and their associated indices and properties are discussed in Table 3.2.1.

Table 3.2.1. Summary of Calibration Parameters, Types and Indices

Parameter Description	Parameter Notation	Type	Index
Relative Spectral Resp.	R	1	B
Scan Mirror Refl. @ bb, sv	r_s (s=bb,sv)	1	B,MS
Scan Mirror Refl. @ ev	r_{ev}	1	B,MS,F
OBC BB emissivity& offset	ϵ_{bb}, T_{bb}	1	B
OBC BB temp correction	T_{bb}	1	B
System non-linearity coef		2	D
System gain or linear coef	m	3	D,S
Background radiance	L_0	3	D,S
System RVS @ EV sector	D_{ev}	4	B,MS
FPA voltage @EV, BB, SV	V_s (s=ev,bb,sv)	3	D,F
Thermistor reading of Temp	T_s (s=mir,bb)	5	S
DN values @ EV, BB, SV	DN_s (s=ev,bb,sv)	5	D,F

where, D=Detector, B=Band, MS=Mirror Side, F=Frame, S=Scan, and
 Type 1: Pre-launch measured or model-estimated variables, represented as Look-Up-Table (LUT).
 Type 2: Pre-launch measured and post-launch interpolated (or extrapolated) variables.
 Type 3: On-line scan-by-scan measured variables.
 Type 4: Off-line measured variables via S/C maneuver observing space through Earth aperture.

Type 5: Telemetry data.

3.2.2 Uncertainty Analysis

The radiometric uncertainty of the MODIS emissive infrared band calibration can be summarized as

$$\frac{L}{L_{Total}} = \sqrt{\underbrace{\frac{Q^2}{Q_{ADC}}}_{\substack{\text{Measured} \\ \text{by SBRS}}} + \underbrace{\frac{L^2}{L_{algorithm}}}_{\substack{\text{algorithm-based} \\ \text{estimate}}} + \underbrace{\frac{L^2}{L_{NIST-BCS}}}_{\substack{\text{NIST-BCS} \\ \text{radiance-transfer}}} + \underbrace{\frac{L^2}{L_{Crosstalk}}}_{\substack{\text{Scene-dependent} \\ \text{(not-included-in-V2.0-L1B)}}} + \frac{L^2}{L_{Scatter}}}. \quad (39)$$

Except the second term, the algorithm-based estimate, all other terms will be characterized and evaluated prelaunch and represented as LUTs. The second term is the sum of all individual contributions of the L1B emissive infrared calibration parameters to the EV radiance calculations; see Table 3.2.1. Those which are evaluated prelaunch will be represented as LUTs; those measured on-orbit will have their uncertainty contributions calculated on per pixel basis. The final uncertainty product will be converted to a dimensionless index value (2^4 gray levels). This arrangement is to provide an efficient as well as space-saving algorithm to calculate the L1B radiance uncertainty product.

A model of MODIS output was generated using a center wavelength based analysis and an estimation of the radiometric uncertainty for each band was then determined for typical scene radiance. Table 3.2.2 and 3.2.3 show a summary of these results for each of the MODIS emissive infrared PV and PC band, respectively. Some of the parameters, w_{cav} , w_{sv} , T_{sam} and T_{swath} , are not listed in Table 3.2.1, because they are associated with stray-light problem, and the magnitude of their contribution needs further investigation, and thus will be discussed in Section 3.2.4. The K_{bb} and e_{bb} in the table correspond to T_{bb} and $\epsilon_{bb} + \epsilon_{bb}$.

Table 3.2.2 Typical Radiance Uncertainty Contributions and RSS Total for PV Bands

	Symbol	Nominal	Perturb.	Band 20	Band 21	Band 22	Band 23	Band 24	Band 25	Band 27	Band 28	Band 29	Band 30
BCS Transfer to BB Temp Adj.	K _{bb}	0 K	Band Dep.	0.55 %	0.53 %	0.53 %	0.52 %	0.46 %	0.47 %	0.29 %	0.26 %	0.22 %	0.21 %
Scan Mirror Temp	T _{mir}	285 K	1 K	0.01 %	0.01 %	0.01 %	0.01 %	0.05 %	0.01 %	0.02 %	0.02 %	0.02 %	0.05 %
BB Temp	T _{bb}	300 K	0.1 K	0.42 %	0.40 %	0.40 %	0.39 %	0.34 %	0.35 %	0.23 %	0.22 %	0.19 %	0.17 %
Scan Cavity Temp	T _{cav}	290 K	10 K	0.21 %	0.21 %	0.21 %	0.21 %	0.19 %	0.19 %	0.08 %	0.06 %	0.04 %	0.05 %
SAM Temp (SV Surround)	T _{sam}	290 K	10 K	0.00 %	0.27 %	0.00 %	0.00 %	2.38 %	0.49 %	0.59 %	0.21 %	0.00 %	0.06 %
BB Earthshine Eff. Temp	T _{swath}	250 K	50 K	0.19 %	0.19 %	0.19 %	0.19 %	0.18 %	0.18 %	0.10 %	0.07 %	0.06 %	0.06 %
Fraction BB Refl. Rad from Cavity	w _{cav}	0.75	-0.25	0.01 %	0.01 %	0.01 %	0.01 %	0.01 %	0.01 %	0.01 %	0.01 %	0.01 %	0.01 %
BCS Transfer to BB Eff. Emiss.	e _{bb}	Band Dep.	0.004	0.01 %	0.01 %	0.01 %	0.01 %	0.01 %	0.01 %	0.01 %	0.01 %	0.01 %	0.01 %
Fraction of SV Rad from SAM	w _{sv}	Band Dep.	0.001	0.01 %	0.06 %	0.01 %	0.01 %	0.51 %	0.10 %	0.37 %	0.20 %	0.01 %	0.13 %
On-Orbit Rel. Refl. Adj. (EV/BB)	D _{ev}	1	0.001	0.10 %	0.17 %	0.09 %	0.09 %	0.77 %	0.10 %	0.61 %	0.32 %	0.05 %	0.21 %
On-Orbit Rel. Refl. Adj. (SV/BB)	D _{sv}	1	0.001	0.04 %	0.11 %	0.04 %	0.04 %	0.82 %	0.15 %	0.65 %	0.36 %	0.01 %	0.25 %
DN (Ltyp)	DN	Band Dep.	Band Dep.	0.03 %	0.31 %	0.03 %	0.03 %	0.12 %	0.04 %	0.07 %	0.04 %	0.02 %	0.03 %
Alpha (2.5% nonlinearity)		Band Dep.	Band Dep.	0.00 %	0.00 %	0.00 %	0.00 %	0.25 %	0.20 %	0.48 %	0.50 %	0.00 %	0.64 %
Center Wavelength		Band Dep.	1 Wave No.	0.29 %	0.33 %	0.33 %	0.33 %	0.25 %	0.26 %	0.14 %	0.10 %	0.06 %	0.00 %
NEdL (Spec.)	NEdL	Band Dep.	Band Dep.	0.21 %	0.63 %	0.28 %	0.28 %	1.29 %	1.05 %	0.93 %	0.79 %	0.09 %	0.59 %
NIST Transfer to BCS (est.)	N/A	N/A	N/A	1.00 %	1.00 %	1.00 %	1.00 %	1.00 %	1.00 %	1.00 %	1.00 %	1.00 %	1.00 %
ADC Nonlinearity (est.)	N/A	N/A	N/A	0.10 %	0.10 %	0.10 %	0.10 %	0.10 %	0.10 %	0.10 %	0.10 %	0.10 %	0.10 %
Crosstalk (Scene Dependent)	N/A	N/A	N/A	N/A	N/A	N/A	N/A	N/A	N/A	N/A	N/A	N/A	N/A
Scatter (Scene Dependent)	N/A	N/A	N/A	N/A	N/A	N/A	N/A	N/A	N/A	N/A	N/A	N/A	N/A
			RSS	1.31 %	1.50 %	1.32 %	1.30 %	3.23 %	1.71 %	1.89 %	1.53 %	1.06 %	1.41 %

Table 3.2.3 Typical Radiance Uncertainty Contributions and RSS Total for PC Bands

	Symbol	Nominal	Perturb.	Band 31	Band 32	Band 33	Band 34	Band 35	Band 36	Band 31hi	Band 32hi
BCS Transfer to BB Temp Adj.	K _{bb}	0 K	Band Dep.	0.19 %	0.19 %	0.20 %	0.21 %	0.22 %	0.23 %	0.19 %	0.19 %
Scan Mirror Temp	T _{mir}	285 K	1 K	0.01 %	0.01 %	0.03 %	0.03 %	0.04 %	0.07 %	0.00 %	0.00 %
BB Temp	T _{bb}	300 K	0.1 K	0.15 %	0.14 %	0.13 %	0.12 %	0.12 %	0.12 %	0.15 %	0.14 %
Scan Cavity Temp	T _{cav}	290 K	10 K	0.05 %	0.06 %	0.08 %	0.09 %	0.10 %	0.11 %	0.05 %	0.06 %
SAM Temp (SV Surround)	T _{sam}	290 K	10 K	0.00 %	0.00 %	0.01 %	0.02 %	0.02 %	0.03 %	0.01 %	0.01 %
BB Earthshine Eff. Temp	T _{swath}	250 K	50 K	0.07 %	0.09 %	0.12 %	0.13 %	0.14 %	0.15 %	0.07 %	0.09 %
Fraction BB Refl. Rad from Cavity	w _{cav}	0.75	-0.25	0.01 %	0.01 %	0.01 %	0.01 %	0.01 %	0.01 %	0.01 %	0.01 %
BCS Transfer to BB Eff. Emiss.	e _{bb}	Band Dep.	0.004	0.01 %	0.01 %	0.01 %	0.01 %	0.01 %	0.01 %	0.01 %	0.01 %
Fraction of SV Rad from SAM	w _{sv}	Band Dep.	0.001	0.01 %	0.01 %	0.06 %	0.08 %	0.12 %	0.21 %	0.07 %	0.07 %
On-Orbit Rel. Refl. Adj. (EV/BB)	D _{ev}	1	0.001	0.04 %	0.04 %	0.09 %	0.14 %	0.20 %	0.38 %	0.15 %	0.14 %
On-Orbit Rel. Refl. Adj. (SV/BB)	D _{sv}	1	0.001	0.01 %	0.01 %	0.12 %	0.17 %	0.23 %	0.41 %	0.12 %	0.11 %
DN (Ltyp)	DN	Band Dep.	Band Dep.	0.02 %	0.02 %	0.02 %	0.02 %	0.03 %	0.04 %	0.01 %	0.01 %
Alpha (2.5% nonlinearity)		Band Dep.	Band Dep.	0.00 %	0.00 %	0.64 %	0.74 %	0.83 %	0.98 %	0.29 %	0.31 %
Center Wavelength		Band Dep.	1 Wave No.	0.09 %	0.13 %	0.20 %	0.22 %	0.22 %	0.22 %	0.09 %	0.13 %
NEdL (Spec.)	NEdL	Band Dep.	Band Dep.	0.07 %	0.07 %	0.40 %	0.43 %	0.45 %	0.74 %	0.64 %	0.54 %
NIST Transfer to BCS (est.)	N/A	N/A	N/A	1.00 %	1.00 %	1.00 %	1.00 %	1.00 %	1.00 %	1.00 %	1.00 %
ADC Nonlinearity (est.)	N/A	N/A	N/A	0.10 %	0.10 %	0.10 %	0.10 %	0.10 %	0.10 %	0.10 %	0.10 %
Crosstalk (Scene Dependent)	N/A	N/A	N/A	N/A	N/A	N/A	N/A	N/A	N/A	N/A	N/A
Scatter (Scene Dependent)	N/A	N/A	N/A	N/A	N/A	N/A	N/A	N/A	N/A	N/A	N/A
			RSS	1.04 %	1.05 %	1.31 %	1.39 %	1.47 %	1.74 %	1.27 %	1.23 %

3.2.3 Constraints, Limitations and Assumptions

The emissive infrared band calibration algorithm assumes an almost perfect instrument without addressing any detector noise (1/f noise in particular) and instrument spurious effects. The MODIS instrument will not likely behave in such ideal way, and the L1B emissive algorithm will have to include many correction terms in order to meet the specification of the emissive infrared band calibration accuracy. However, the algorithm described above represents a relatively well understood “clean” part of the MODIS instrument. However detector noise and instrument spurious effects still need further investigation and model-validation using both the prelaunch thermal vacuum test data and postlaunch data before a complete and working correction algorithm can be developed.

In this section, a preliminary algorithm for the 1/f noise correction and instrument spurious source corrections will be discussed based on our current understanding of the problems.

3.2.3.1 Detector 1/f Noise Correction

The MODIS raw output is a small, rapidly varying signal superimposed on a large background that varies more slowly, due to the thermal drifts and 1/f noise. Like its predecessor instruments, MODIS views space as its background subtraction reference and a full-aperture blackbody as its second reference for calibration. MODIS measures space and blackbody reference before and after each Earth view scan line. If 1/f noise is known at the time MODIS is viewing the space and blackbody reference then 1/f noise in the Earth view sector can be interpolated between four known reference values, that is, two points before and after the current Earth view scan line.

If the 1/f noise is to be included, the top level calibration equation 31 must be rewritten as

$$V_s = \alpha m^2 (L_s + L_0)^2 + m(L_s + L_0) + V_n, \quad (40)$$

where V_n stands for the 1/f noise correction. Eqs.33-35 must then contain V_n in such a way that V_s (where s can be either bb or sv or ev) is replaced by $V_s - V_n$. Averaging m and L_0 over many scans will suppress the noise and yield a relatively 1/f noise-free system gain \bar{m} and background radiance \bar{L}_0 . Substitution of \bar{m} and \bar{L}_0 into Eq.40 for the BB and SV measurements yields two solutions for V_n at the time MODIS is viewing the blackbody and space,

$$V_n(t_1) = V_{bb} - \alpha \bar{m}^2 (L_{bb} + \bar{L}_0)^2 - \bar{m} (L_{bb} + \bar{L}_0), \quad (41)$$

$$V_n(t_2) = V_{sv} - \alpha \bar{m}^2 (L_{sv} + \bar{L}_0)^2 - \bar{m} (L_{sv} + \bar{L}_0), \quad (42)$$

where $t_2 - t_1 = 0.122$ (s), the timing difference between the two views. These are the two known 1/f values before the Earth view scan line. Similarly, $V_n(t_3)$ and $V_n(t_4)$ are the BB and SV values after the current Earth view scan line, where $t_3 - t_1 = 2.954$ (s), the time for a complete rotation of the scan mirror. Here the two mirror sides are treated separately. The 1/f noise V_n for the Earth view sector will be interpolated between these four points $V_n(t_i)$ ($i=1,2,3,4$).

3.2.3.2 Instrument Spurious Source Corrections

In general, each of the measured at-aperture radiance terms (L_{ev} , L_{sv} , L_{bb}) can be contaminated by radiation from sources other than the nominal “within-the-Field-of-view” scene radiance. These spurious contamination sources, to the extent that they are determined by characterization or modeling to be significant, can be accounted for by substitution:

$$L'_{ev} \rightarrow L_{ev} + L^{ev}_{emiss}(T_{cav}) + L^{ev}_{scene_refl}(T_{scene}) \quad (43)$$

$$L'_{sv} \rightarrow L_{sv} + L^{sv}_{emiss}(T_{cav}) + L^{sv}_{scene_refl}(T_{scene}) \quad (44)$$

$$L'_{bb} \rightarrow L_{bb} + L^{bb}_{emiss}(T_{cav}) + L^{bb}_{scene_refl}(T_{scene}) \quad (45)$$

where the first terms on the right-hand-side designate the nominal (intended) radiance, L_{emiss} and L_{scene_refl} represent the radiance from cavity emission sources and scene radiance sources scattered or reflected into the MODIS FOV, and T_{cav} and T_{scene} represent the scan cavity and scene temperatures, respectively.

A full and detailed list of cavity emission and Earth scene spurious radiance sources, which can have the path scattered or reflected into the MODIS FOV, can be found in the Appendix.

During the spacecraft maneuver to view deep space through the Earth aperture, the Earth scene spurious radiance source terms will be absent, enabling measurement of the cavity emission spurious source terms. To the extent that cavity temperature dependent contamination source terms are measurable as a result of the deep space view maneuver, corrections terms can be incorporated into the algorithm. Unique measurement of the scene temperature dependent terms is more difficult. This will require careful assessment of instrument performance in response to specific scene contrast features.

Preliminary analyses indicate that the effects of some of these spurious terms are negligible; others are still to be determined (using PFM test data) and therefore not included in the current correction algorithm. The current correction algorithm uses a simpler version of Eqs. 43-45,

$$L'_{ev} \rightarrow L_{ev} , \quad (46)$$

$$L'_{sv} \rightarrow L_{sv} + L^{sv}_{emiss}(T_{cav}) , \quad (47)$$

$$L'_{bb} \rightarrow L_{bb} + L^{bb}_{emiss}(T_{cav}) + L^{bb}_{scene_refl}(T_{scene}) \quad (48)$$

The correction term identified for the space view (Eq.47) is incorporated as a weighting factor applied to the Planck function for the space view surround temperature, characterized by the temperature of the Space Analog Module (SAM) electronics, T_{SAM}

$$L'_{sv} \rightarrow L_{sv} + w_{sam} L_{cav}(T_{SAM}) \quad (49)$$

where w_{sam} is determined initially from modeling estimates.

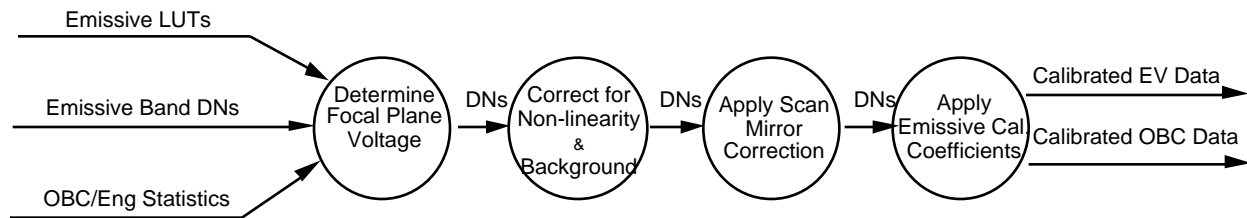
The correction terms identified for the BB are incorporated as weighting factors applied to the Planck function for the cavity and scene temperature, respectively,

$$L'_{bb} \rightarrow L_{bb} + w_{cav}L_{cav}(T_{cav}) + w_{scene}L_{scene}(T_{scene}) \quad (50)$$

where w_{cav} and w_{scene} are determined initially from modeling estimates. This formulation treats the blackbody reflection of scene radiance into the MODIS FOV as an effective diffuse process, thus enabling a simpler correction process.

3.2.4 Practical Considerations

The L1B emissive band calibration data flow diagram is:



3.2.4.1 Programming Considerations

The software implementation of the algorithm takes into consideration efficient use of computing resources and ease of maintenance in the production environment. The software system makes extensive use of look-up tables generated in the CROM instead of direct computations in the production system. This technique reduces CPU requirements in the production environment by moving computation of stable or slowly varying terms out of the time-critical production stream. Changes to instrument characteristics or to the way these characteristics are determined are provided as updated input datasets rather than new versions or releases of the production software. These tables are sized to include expected parameter ranges with a resolution determined to minimize both interpolation errors and software memory use.

3.2.4.2 Quality Control and Diagnostics

The Level 1B production software monitors and reports many IR sensitive conditions such as: high blackbody / scan cavity temperature differential, SRCA on, SD illuminated, blackbody heater on, moon in space view, excessive negative Earth scene radiance, less than 6 blackbody thermistors used, less than 9 blackbody frames used, and less than 9 space view frames used. Messages describing these conditions are written to the message logs using the Status Messaging Facility (SMF) supported in the Science Data Processing Tool Kit (SDPTK). The Level 1B Product Specification describes a set of conditions for which data is marked as suspect, and a set of QA flags which provide additional information.

3.2.4.3 Exception Handling

An outlier rejection routine will be applied to the blackbody and space view data every scan to preclude any anomalous data points attributable to phenomena such as electronic glitches or charged particles. The outlier rejection routine will also be applied to the twelve blackbody thermistors.

Lunar viewing through the space view will temporarily cause this source to be unusable. Because the duration of this event is expected to be on the order of 10 scans, the thermal offset and noise

correction term will be determined only from the blackbody signals. For the PC bands (bands 31-36) electronic calibration will also render the SV data unusable.

3.2.4.4 Output Product

The Level 1B emissive band product consists of the apparent Earth scene spectral radiance for each scene pixel. The output product also includes a dimensionless uncertainty index for each pixel. A conversion table which can be used to transform this radiometric product to an effective scene temperature will be available as a separate product from the GSFC DAAC. Negative radiance values attributed to noise suppression and space view surround radiance can occur. These negative values are useful for subsequent analysis and will be carried and not converted to zero.

3.3 The Spectroradiometric Calibration Assembly (SRCA)

The SRCA is a partial aperture, multi-mode (radiometric, spectral, spatial) calibration instrument that provides spectral calibration of the VIS and NIR bands and radiometric calibration of the VIS, NIR, and SWIR bands. In addition the SRCA can track the band-to-band registration of the bands and establish geometric coregistration of them along track and along scan. It provides a transfer of the prelaunch laboratory radiometric calibration (in the VIS/NIR/SWIR) to orbit for the solar diffuser.

3.3.1 The Radiometric Mode

The objectives of the SRCA radiometric mode are:

- 1) Track changes in MODIS reflective band radiometric calibration from prelaunch to on-orbit.
- 2) Track changes in radiometric characteristics within orbit.

Different radiance levels are necessary for calibrating the MODIS bands at appropriate signal levels. Six levels are available. Six lamps (four 10W and two 1W) are embedded in the Spherical Integrating Sphere (SIS). Four of them are used to provide different output radiance levels and the other two, one 10W and one 1W, are backups. The combination of three 10W lamps and one 1W lamp provides four light levels (three 10W, two 10W, one 10W, and one 1W). Insertion of a neutral density (ND) filter (transmittance = 0.25) for the one 10W and one 1W cases provides two additional light levels.

The SRCA source is normally operated in constant radiance mode. There are two temperature-controlled silicon photodiode (SiPD) (one primary, one backup) embedded in the SRCA SIS. The operational SiPD measures the variations in the wavelength integrated radiance at the SIS wall. The output of the SiPD is amplified and used to adjust the lamp current. The feedback control circuit keeps the broadband radiance output from the SRCA source constant. The SRCA source is switched to constant current mode when one of the most frequently used lamps (one 10W or 1W) fails. Constant current mode will then be used to the end of MODIS life.

The baseline on-board radiometric calibration for the VIS, NIR, and SWIR, MODIS bands 1 - 19 and 26, is accomplished as follows.

The laboratory spherical integration source SIS(100) is traceable to the NIST standard. Error in the transfer from the SIS(100) to the SRCA increases the uncertainty to 3.6% due to uncertainties in center wavelength shift, crosstalk, out-of-band response, polarization, non-linearity, and stray light, among other factors.

The SRCA transfers the calibration to space after launch. The SRCA will transfer the calibration to

the SD/SDSM during the A&E phase with an anticipated overall radiometric uncertainty of 4.0%.

3.3.2 The Spectral Mode

The Spectral mode is used to characterize spectral shifts in the reflected solar reflective bands. Evidence from precursor instruments suggests that such spectral shifts can occur during insertion into orbit and during on-orbit operations. The spectral response of the MODIS system is measured prelaunch for all bands, using an external double monochromator/collimator system which fills the full MODIS aperture.

The MODIS spectral filters for the reflected solar bands are of the Ion-Assisted Deposition (IAD) filters which are thought to be less susceptible to air-to-vacuum (launch) shifts. The beam splitter dichroics are not of the IAD type so spectral shifts might yet be observed. Prelaunch thermal vacuum testing may answer this question.

In the spectral calibration mode, the entrance and exit slits and the grating are employed. Three order-sorting filters plus one open position (with no filter) are switched in and out according to the grating angle and the diffraction order used. Unlike the radiometric calibration mode, only two light levels are used for the SRCA SIS output in spectral mode (three 10W and one 10W).

The SRCA has the capability of wavelength self-calibration. Didymium absorption glass is used as the wavelength calibrator. The signals from the calibration detector behind the didymium glass, after normalization by the reference detector signals, are used to determine two monochromator parameters. The spectral calibration is operable for VIS, NIR, and SWIR bands (1-19, 26) although it is less accurate for $> 1 \mu\text{m}$.

There is no demonstrated method for validating the spectral characteristics of MODIS using on-orbit ground verification methods.

3.3.3 The Spatial Mode

The spatial location accuracy has two aspects: (1) the accuracy of the geolocation for a single reference band, and (2) the accuracy of the coregistration of other bands relative to the reference band. The geolocation accuracy will be improved by SDST during the A&E phase by analyzing scenes.

During prelaunch activities Ground Support Equipment (GSE) measures the position along scan and along track of each MODIS detector. The SRCA also measures the apparent relative position along-scan for each detector and the centroid position along-track for each band. These data are used to spatially calibrate the SRCA against the GSE. Correction coefficients are introduced to account for the partial illumination SRCA aperture. The GSE data are also used to check for specification compliance.

During on-orbit activities the SRCA senses the relative position shifts in the along-scan direction for each detector and the centroid shifts in the along-track direction for each band. The misregistration is computed using on-orbit data and comparing it with the pre-launch detector position.

The 490 detectors for 36 MODIS bands are located on four different focal planes. The measurement resolution for the relative detector position by the GSE is expected to be 1/40 of the detector size. There could be relative shifts between the focal planes after launch, but the relative

shifts of any detectors within a focal plane should be negligible.

When the SRCA is used in the spatial mode, the SRCA infrared source is heated to $390\text{K} \pm 5\text{K}$. Four SIS lamp configurations are used: three 10W, two 10W, one 10W and one 1W. A dichroic beam combiner in the filter wheel is selected, which combines the VIS/NIR /SWIR beam from the SRCA SIS with the infrared beam from the thermal source. For spatial measurements a plain mirror replaces the grating in the monochrometer. As various lamp combinations are introduced, the reticle motor alternately locates the along-scan reticle and the along-track reticle into the optical path. The reticles, illuminated by the light sources, are imaged onto the MODIS focal planes. The reticle image is scanned across the MODIS detectors as the MODIS scan mirror rotates. The signals for different frames and electronic phase-delay settings are collected by the MODIS detectors, which provide the data for determining the relative position shifts of detectors (bands) on-orbit.

Details of the SRCA and the calibration algorithm are documented in [Montgomery and Che, 1996].

3.4 Vicarious Calibration

3.4.1 An Overview

MODIS has a set of challenging requirements for radiometry and for other measurements (see appendix C). These requirements are imposed by the science needs of the level 2, 3, and 4 products derived from MODIS. In order to assure these science needs are met it is most beneficial to have available several independent methods to establish and verify important components of the instrument calibration throughout the mission. It is vicarious calibration (VC) that provides the critical independent determinations of radiance or reflectance at the MODIS aperture for a given detector at a specific time. Combining ground/aircraft radiance measurements with the instrument response in counts provides the independent responsivity determinations needed to verify or modify the MODIS calibration.

Vicarious methods are reliable because they exercise the operational imaging mode of the sensor and implicitly account for size of source effects. However such calibrations are made much less frequently than on-orbit calibrations and usually yield much fewer data points (order of magnitude of 10 TOA radiances per field campaign).

3.4.1.1 The Fundamental Concept

The fundamental concept of vicarious calibration is measurement of scene radiance at the top of the atmosphere with instruments other than MODIS, within a specific MODIS band, and identified with a specific pixel of a MODIS observation. Each VC determination of absolute TOA radiance also will include an estimate of the uncertainty. In each instance spatial and spectral registration must be followed carefully to obtain useful results.

There are numerous vicarious calibration techniques in both the reflected [Slater *et al.*, 1987] and thermal [King *et al.*, 1995] bands. They include ground [Slater *et al.*, 1995], aircraft [Abel *et al.*, 1993], buoy [McClain *et al.*, 1992] and lunar [Kieffer and Widley, 1992] observations.

Vicarious calibration will be accomplished using three methods: the reflectance method; the radiance method; and the comparison method.

The reflectance based method provides calibration results relative to the sun. The reflectance calibration is done as follows. Measurements of reflectance at the ground site and measurements of atmospheric properties are made at the time of the MODIS overpass. These measurements are input to a radiative transfer code and the TOA radiance is computed. These radiance values are combined with digital counts derived from the MODIS image data to derive a set of calibration coefficients which are then compared to the stored set of coefficients. Because of the large area of the MODIS footprint it is not possible to measure the entire reflectance function on the ground. Instead a conveniently sized area will be measured on the ground and compared to the same area measured from an aircraft or other satellite instrument. Aircraft or satellite based measurements then will be used to scale up to the area covered by several MODIS pixels. The number of pixels calibrated in any type of VC measurement is, of course, limited by the uniformity of the site.

The radiance based method is usually partitioned into high altitude (~20km) experiments and low altitude (0.2km to 3km above sea level) experiments. The method is used, in part, as an independent source of data to validate the performance of the on-board calibrators. The radiance calibration is done as follows. Aircraft based measurements of radiance are made of the site and the atmospheric properties above the site are measured by ground instruments. The radiative transfer code is used to determine the effect of the atmosphere above the aircraft and the absolute radiance at the TOA is obtained. As before, these radiance values are combined with digital counts derived from MODIS image data to derive a set of calibration coefficients.

The high altitude method demands an accurate prediction of the satellite-target viewing geometry because of the necessity of coaligning the aircraft measurement vector with the satellite view vector during a MODIS overpass. Corrections must be applied to account for differences in footprint size of the two instruments. The need for atmospheric correction is minimized because the aircraft is operated in the stratosphere. However corrections still are needed for stratosphere ozone and stratosphere aerosols.

The low altitude option is logistically simpler and less expensive. However, the atmospheric correction problem is more demanding.

The comparison method two or more independent satellite sensors which image the same ground scene. The first problem to be accounted for is the registration of sensor A's pixels and the MODIS pixels. The second problem is that sensor A digital counts and its calibration coefficients must be combined to produce TOA radiances; the same is done for MODIS. Either the TOA radiance data of sensor A are resampled (or, if smaller, summed) to match areas sampled by the MODIS pixels or vice versa. The spectral bands of sensor A and MODIS may be different and a correction must be derived from the spectral reflectance of the site in order to convert the radiance measured by sensor A to that of a similar MODIS band.

The Moon is the only object accessible to terrestrial-orbiting spacecraft that is within the dynamic range of most imaging instruments and is stable enough to provide a potential calibration target. Although the Moon itself is extremely stable, its photometric properties are neither spatially uniform nor near to lambertian. Also, the small change in apparent orientation (libration) must be considered. The present radiometric knowledge of the lunar brightness is on the order of 15%, not adequate to provide good radiometric calibration. A ground-based telescope program is underway with the objective of characterizing lunar brightness with an accuracy of about 2%.

Lunar calibration requires two activities; characterization of lunar brightness, which is common to all spacecraft and instruments, and ASTER and MODIS observations of the Moon. The objective of the telescope program at the University of Arizona is to develop radiometric knowledge of the Moon adequate to support calibration of a variety of current and anticipated spacecraft imaging instruments. The specific goal is the development of a radiometric model at a number of

wavelengths in the 0.4 μm to 2.5 μm region with an angular resolution of 5 arc-seconds covering the full range of lunar libration over all phase angles between onset of eclipse and 90 degrees.

ASTER and MODIS are calibrated by acquiring lunar images in all solar bands with the Moon at less than 90 degrees phase. The data are processed to the normal Level 1 radiometric product and compared with the absolute lunar radiance model. The space port will view the moon at 67 degree phase angle several months of each year with the platform in its normal nadir orientation. Direct viewing by reorientation of the platform is highly desirable.

Lunar vicarious measurements are processed differently. Lunar data are collected through the SV port rather than the EV port. When the center of the moon comes within an angle θ_{moon} of the edge of the SV port the data processing starts lunar mode. Here, θ_{moon} has units of degrees and will be calculated as half of the lunar radius plus an estimate of the angular distance needed so that far field scatter into the SV port is less than half the NEdL of the most sensitive channel of MODIS (an angle equivalent to about 5 pixels).

When lunar mode starts, the zero radiance level determined from the SV will be frozen and maintained for the duration of the lunar mode, during which time the DN values of the SV data will be treated like EV data. Radiance and reflectance values will be calculated, applying the standard calibration formulas with the current responsivities in both the reflected and emitted bands plus the frozen background subtraction values. Radiance and reflectance uncertainty estimates will also be calculated in the same way that they are calculated for EV data.

3.4.1.2 Vicarious Calibration and the MCST Strategy

The application of vicarious calibration measurements to the MODIS reflective band calibration algorithm is accomplished via the multiplicative correction factors, $F_{\text{VC,LB}}$ (Eq 5) and $F_{\text{VC,E}}$ (Eq 6). In the thermal bands the information from vicarious calibration will be used to change the band emissivity of the BB or used to change additive temperature offsets of the average BB and cavity temperatures. This approach is based on the expectation that vicarious calibrations are more useful for checking overall radiometric scales. More sophisticated techniques are needed for tracking linearity, spectral shifts or angle corrections.

After launch, MCST will convene a panel of experts (primarily users of the L1B product) to review the instrument calibration status. This panel will include experts in both reflected band and emitted band vicarious calibration techniques, experts on the characteristics and preflight calibration of the MODIS instrument, and MCST members familiar with the algorithms used in the Level 1B MODIS processing.

The panel will review responsivities as functions of time for all of the bands as determined by the OBCs and by vicarious data sets. Useful data sets will be those shown to possess internal consistency, that include uncertainty estimates, and are traceable to NIST or other EOS approved standards.

Before changes are introduced in the MODIS calibration and characterization parameters MCST will test the impact of these changes on the upper level products. These changes will be checked through the use of test data sets distributed to Level 1B product users.

The panel of experts represent the Science Team. The panel will provide recommendations to the Science Team Leader. Implementation of the changes to the algorithm and calibration parameters is the responsibility of the MCST Leader working for the Science Team Leader.

3.4.1.3 Uncertainty Estimates

The primary contribution to the uncertainty estimate for vicarious calibration is provided with those data sets. Since most vicarious calibration techniques are derived from peer reviewed and published techniques, the uncertainty estimates are expected to be faithful to the individual measurements provided. In the use of these data sets each specific comparison will be reviewed by MCST to verify the applicability of the typical uncertainty budget for this specific instance of application.

3.4.2 Practical Considerations

3.4.2.1 Programming Considerations

A table of F_{VC} values for the reflected solar bands will be read into the algorithm. Similarly the emissivity table will be read in at the start of L1B processing and applied in the thermal algorithms. The corresponding uncertainty values will be read into the algorithm as tables.

3.4.2.2 Vicarious Calibration and Validation

Reviews of the available data sets by the MODIS Science Team validation panel provides the validation of the L1B product.

3.4.2.3 Quality Control, Diagnostics and Exception Handling

Vicarious calibration analyses and processing are accomplished offline.

3.5 Calibrating the Engineering Telemetry Data

3.5.1 Theoretical Description

The MODIS instrument data stream includes the science data that are used for radiance determinations. It also includes hundreds of engineering sensor readings from the instrument including internal temperatures, voltages, currents, and other health and safety measurements. These engineering data are converted from counts to engineering units as part of the MODIS L1B processing.

3.5.1.1 Mathematical Description of Algorithm

All engineering count data are converted into engineering units using a 5th order polynomial. The polynomial coefficients for each sensor will be determined by ground testing [Mehrten, 1995]. The coefficients are entered into the L1B algorithm as a table. Some of the temperature sensors in the cooled focal planes have three sets of coefficients. The selection of the appropriate set of coefficients is determined by the temperature set point for the focal planes. An alternative approach will be developed for the focal planes when they are operated "open loop".

3.5.1.2 Uncertainty Estimates

The uncertainty estimates will be derived from the variance of the residuals that fit the ground measurements.

3.5.2 Practical Considerations

3.5.2.1 Quality Control and Diagnostics

Along with the polynomial coefficients, each sensor will have upper and lower alarm limits specified in engineering units. If the measured parameter falls outside the limits then a message listing the spacecraft time of the measurement, the sensor, the measurement, and the exceeded limit will be entered into the MODIS log. A sensor exceeding a limit within a processing run will be recorded as a single event in the log. All the scan lines containing a limit that has been exceeded will be flagged with a warning in the data product. Processing will not be interrupted by these alarms and flags.

3.5.2.2 Exception Handling

All detector measurements will be checked against a list of dead and noisy detectors. This list will be created from ground test data. The measurements from dead detectors will be filled with a flag value. Dead detectors will not be flagged for exceeding alarm limits. The list will be modified with flight observations.

3.5.2.3 Output Product

Each engineering sensor reading in the L1A data product will be converted to engineering units in the L1B data product.

4. ISSUES TO BE ADDRESSED

There are several subject matters that must be addressed to be better prepared for flight operations and for handling of satellite data.

(1) A fundamental assumption implicit throughout this document is that the MODIS instrument will perform substantially as originally specified [Weber, 1993]. In particular it is assumed that spurious effects (scatter, ghosting, cross talk, out of band response) will be small. There are no corrections to the radiance estimate of a detector based on the radiance measurements in other pixels or bands. Similarly, the uncertainty estimates for radiance and reflectance do not include these scene dependent terms. The magnitude of the radiance uncertainties and the possibilities for correct algorithms are under active investigation.

(2) The EM of MODIS has been tested. The results of the tests show the aberrations expected for a test model but do not include the SRCA or SD/SDSM modules. The PFM testing is not complete at this writing. Many assumptions made this year will be validated with the results of PFM tests.

(3) Some modeling has been performed to develop an algorithm for relative intra-band radiometric calibration based on the overlapping FOVs of the MODIS detectors, also known as the bowtie effect. Enhancement of this model will continue into 1997, but will not be included in the Version 2.0 software.

(4) Image based relative calibration techniques that do not use the bowtie effect will not be in the Version 2.0 software.

(5) Calibrations using spacecraft maneuvers have been investigated during the past year. As of this writing, a specific set of maneuvers has not been accepted by the AM project office. It is expected that a decision and procedures for using the data from such maneuvers will be incorporated into the Version 2.1 software

(6) MODIS has redundant power supplies, amplifiers, and other electronic components. It has been assumed that the calibration of the detectors will be same for the primary and secondary electronics. A determination of the validity of this assumption will be made during ground testing. If the assumption does not hold, changes will be made to reflect the specific choices of infraredcuietry; these choices will be documented in the 1997 version of the ATBD.

(7) MODIS has the ability to change gain settings for the PV bands by command from the ground. The protocols to do this and maintain a consistent calibration scale are not complete. No telemetered changes in gain were assumed in this 1996 version ATBD.

(8) The ground calibration of MODIS solar reflected bands with large atmospheric water absorption cross sections is expected to have large uncertainties; such uncertainties have not been addressed in this document.

5. APPENDIX A: PEER REVIEW BOARD ACCEPTANCE REPORT

This page intentional left blank

6. APPENDIX B: MODIS SPECTRAL BANDS SPECIFICATION

BAND		IFOV	Bandwidth	PURPOSE (Examples)
LAND AND CLOUD BOUNDARIES/PROPERTIES BANDS				
1	645 nm	250 m	50 nm	Veg. Chlorophyll Absorption
2	858 nm	250 m	35 nm	Cloud and Veg. Land Cover Transformation
3	469 nm	500 m	20 nm	Soil, Vegetation Differences
4	555 nm	500 m	20 nm	Green Vegetation
5	1240 nm	500 m	20 nm	Leaf/Canopy Differences
6	1640 nm	500 m	24.6 nm	Snow/Cloud Differences
7	2130 nm	500 m	50 nm	Land and Cloud Properties
OCEAN COLOR BANDS				
8	412 nm	1000 m	15 nm	Chlorophyll
9	443 nm	1000 m	10 nm	Chlorophyll
10	488 nm	1000 m	10 nm	Chlorophyll
11	531 nm	1000 m	10 nm	Chlorophyll
12	551 nm	1000 m	10 nm	Sediments
13	667 nm	1000 m	10 nm	Sediments, Atmosphere
14	678 nm	1000 m	10 nm	Chlorophyll Fluorescence
15	748 nm	1000 m	10 nm	Aerosol Properties
16	869 nm	1000 m	15 nm	Aerosol/Atmospheric Properties
ATMOSPHERE/CLOUD BANDS				
17	905 nm	1000 m	30 nm	Cloud/Atmospheric Properties
18	936 nm	1000 m	10 nm	Cloud/Atmospheric Properties
19	940 nm	1000 m	50 nm	Cloud/Atmospheric Properties
THERMAL BANDS				
20	3.75 μm	1000 m	0.18 μm	Sea Surface Temperature
21	3.96 μm	1000 m	0.059 μm	Forest Finfraredes/Volcanoes
22	3.96 μm	1000 m	0.059 μm	Cloud/Surface Temperature
23	4.05 μm	1000 m	0.061 μm	Cloud/Surface Temperature
24	4.47 μm	1000 m	0.065 μm	Tropospheric Temperature/Cloud Fraction
25	4.52 μm	1000 m	0.067 μm	Tropospheric Temperature/Cloud Fraction
26	1375 nm	1000 m	30 nm	Cinfraredrus Cloud Detection
27	6.72 μm	1000 m	0.36 μm	Mid-Tropospheric Humidity
28	7.33 μm	1000 m	0.30 μm	Upper-Tropospheric Humidity
29	8.55 μm	1000 m	0.30 μm	Surface Temperature
30	9.73 μm	1000 m	0.30 μm	Total Ozone
31	11.03 μm	1000 m	0.50 μm	Cloud/Surface Temperature
THERMAL BANDS				
32	12.02 μm	1000 m	0.50 μm	Cloud Height & Surface Temperature
33	13.34 μm	1000 m	0.30 μm	Cloud Height & Fraction
34	13.64 μm	1000 m	0.30 μm	Cloud Height & Fraction
35	13.94 μm	1000 m	0.30 μm	Cloud Height & Fraction
36	14.24 μm	1000 m	0.30 μm	Cloud Height & Fraction

7. APPENDIX C: KEY MODIS REQUIREMENTS

Absolute radiometric calibration accuracy (1σ @ L_{typ}) with uniform scenes		
<3 μ m	$\pm 5\%$	
>3 μ m, except bands 20, 21, 31, 32	$\pm 1\%$	
Band 20 (3.75 μ m)	$\pm 0.75\%$	(Goal $\pm 0.5\%$)
Bands 31 (11.03 μ m) & 32 (12.02 μ m)	$\pm 0.5\%$	(Goal $\pm 0.25\%$)
"High" band 21 (3.96 μ m)	$\pm 10\%$	(Agreed w/ SBRC) --Not in Spec
"High" bands 31hi, 32hi	$\pm 10\%$	
Reflectance (Target r at TOA)	$\pm 2\%$	
Stability of Radiance Ratio		
Ratio of mean band responses (max change in two week interval)	$\pm 0.5\%$ @ full scale $\pm 1\%$ @ half scale	
Spectral Characterization Accuracy		
$\leq \lambda_0$	preflight $\pm 0.5\text{nm}$	where
$> \lambda_0$	preflight $\pm 0.5(\lambda / \lambda_0)\text{nm}$	$\lambda_0 = 1.0\mu\text{m}$
$< \lambda_1$	on-orbit $\pm 1.0(\lambda / \lambda_1)\text{nm}$	$\lambda_1 = 0.412\mu\text{m}$
Spatial Characterization		
MODIS Pointing Knowledge with reference to EOS AM-1	± 30 arcseconds, 1 σ ($\pm 100\text{m}$ at nadir)	
Absolute AM-1 pointing knowledge	± 30 arcseconds, 1 σ ($\pm 100\text{m}$ at nadir)	
Coregistration		
1 km \rightarrow	1 km	± 0.2 km (goal ± 0.1 km)
0.5 km \rightarrow	0.5 km	± 0.1 km (goal ± 0.05 km)
0.25 km \rightarrow	0.25 km	± 0.05 km (goal ± 0.025 km)
1 km \rightarrow	0.5 km	± 0.2 km (goal ± 0.1 km)
1 km \rightarrow	0.25 km	± 0.2 km (goal ± 0.1 km)
Bright Target Recovery & Associated Optical Effects		
L _{cloud} \rightarrow	L _{typ} (Reflective Bands)	Output settles to $< \pm 0.5\%$
L _{max} \rightarrow	L _{typ} (Thermal Bands)	within 2 km of entering L _{typ} regime

8. APPENDIX D: ACRONYMS AND ABBREVIATIONS

A/D	Analog-to-Digital Converter
A&E	Activation and Evaluation
AM-1	Ante Meridian EOS Platform
ATBD	Algorithm Theoretical Basis Document
AU	Astronomical Unit
AVHRR	Advanced Very High Resolution Radiometer
BB	OBC Blackbody
BCS	Blackbody Calibration Source
BRDF	Bi-Dinfraredirectional Reflectance Distribution Function
BRF	Bi-Dinfraredirectional Reflectance Factor
CARF	Combined Aperture Response Function
CARFS	CARF along-scan
CARFT	CARF along-track
CDR	Critical Design Review
CZCS	Coastal Zone Color Scanner
DAAC	Distributed Active Archive Center
DC	Dinfraredect Current
DN	Digital Number
EM	Engineering Model
EOS	Earth Observing System
EV	Earth view
FPA	Focal Plane Assembly
GSE	Ground Support Equipment
HINFRAREDS	High Resolution Infrared Spectrometer
IAC	Integration Alignment Collimator
IFOV	Instantaneous Field of View
INFRARED	Infrared
K	Kelvin
LWINFRARED	Long Wavelength Infrared
MCST	MODIS Characterization Support Team
MODIS	Moderate-Resolution Imaging Spectroradiometer
MTPE	Mission to Planet Earth
MWINFRARED	Medium Wavelength Infrared
NASA	National Aeronautics and Space Administration
NINFRARED	Near Infrared
NIST	National Institute of Standards and Technology
nm	Nanometers (10^9 meters)
ND	Neutral Density
NOAA	National Oceanic and Atmospheric Administration
NOSC	Naval Ocean Systems Center
OBC	On-Board Calibrator
OOB	Out-of-Band
PC	Photoconductive
PM-1	Post Meridian EOS Platform
PV	Photovoltaic
RSS	Root-Sum-Square
SAM	Space Analog Module
SBRS	Santa Barbara Remote Sensing
SD	Solar Diffuser
SDSM	Solar Diffuser Stability Monitor

SDST	Science Data Support Team
SeaWiFS	Sea Viewing Wide Field of View Sensor
SiPD	Silicon Photodiode
SIS	Spherical Integrating Source
SNR	Signal-to-Noise Ratio
SPMA	Spectral Measurement Assembly
SRCA	Spectroradiometric Calibration Assembly
SV	Space View
SWINFRARED	Short Wavelength Infrared
TAC	Test Analysis Controller
TBD	to be determined
TDI	Time Delay Integration
TLCF	Team Leader Computing Facility
TM	Thematic Mapper
TOA	Top of the Atmosphere
TRMM	Tropical Rainfall Measuring Mission
TV	Thermal Vacuum
USGCRP	U.S. Global Change Research Program
VIS	Visible

9. APPENDIX E: REFERENCES

- Abel, P., B. Guenther, R. Galimore, and J. Cooper, Calibration results for NOAA-11 AVHRR channels 1 and 2 from congruent infraredcraft observations, *J. Atmos. and Ocean. Technol.*, 10, 493-508, 1993.
- Barbieri, R., and B. Guenther, The MCST Management Plan, NASA Goddard Space Flight Center, Greenbelt MD, 1995.
- Barker, J., J. Harnden, H. Montgomery, P. Anuta, G. Kvaran, E. Knight, T. Bryant, A. McKay, J. Smid, and D. Knowles, MODIS Level 1 Geolocation, Characterization and Calibration Algorithm theoretical Basis Document, Version 1, Goddard Space Flight Center, Greenbelt MD, 1994.
- Barnes, R., A. Holmes, W. Barnes, W. Esaias, and C. McClain, SeaWifs Prelaunch Radiometric Calibration and Spectral Characterization, NASA TM 104566, vol 23, October 1994.
- Bremer, J., Optimization of the GOES-I Imager's radiometric accuracy: drift and 1/f noise suppression, *Optical Eng.*, 33 (10), 1994.
- EOS, Functional and Performance Requirements Specification for the Earth Observing System Data and Information System (EOSDIS) Core System, NASA, 1994.
- Goldberg, I.L., Two-point calibration of non-linear PC HgCdTe channels, *Infrared Phys. Technol.*, 36, 1995.
- Guenther, B. ed. The MODIS Calibration Plan Version 2, GSFC, 1995.
- Guenther, B., H. Montgomery, P. Abel, J. Barker, W. Barnes, P. Anuta, J. Baden, L. Carpenter, E. Knight, G. Godden, M. Hopkins, M. Jones, D. Knowles, S. Sinkfield, B. Veiga, N. Che, L. Goldberg, M. Maxwell, T. Zukowski, T. Pagano, N. Therrien, and J. Young, MODIS Level 1B Algorithm Theoretical Basis Document [MOD-02], GSFC, Greenbelt Maryland, 1995.
- Guenther, B., W. Barnes, E. Knight, J. Barker, J. Harnden, G. Godden, H. Montgomery, and P. Abel, MODIS Calibration: A Brief Review of the Strategy for the At-Launch Calibration Approach, *J. Atmos Ocean. Tech.*, 13, 274-285, 1996.
- Hopkins, M., J. Baden, and J. Hannon, MODIS Level 1B Data Product Format, General Science Corporation, Seabrook MD, 1995a.
- Hopkins, M., J. Hannon, and J. Baden, MODIS Level 1B Software Design Document, General Sciences Corporation, Seabrook MD, 1995b.
- Kieffer, H.H., and R.L. Widley, Spectrophotometry of the Moon for Calibration of Spaceborne Imaging Instruments, in *Lunar and Planetary Science Conference 23*, pp. 687-688, 1992.
- Kieffer, H.H., and R.L. Widley, Establishing the Moon as a Spectral Radiance Standard, *J. Atmos Ocean. Tech.*, 13, 360-375, 1996.
- King, M., Letter to John Parslow of CSINFRAREDO, 6 January 1994.
- King, M., W.P. Menzel, P. Grant, J. Myers, G.T. Arnold, S. Platnick, L. Gumley, S. Tsay, C. Moeller, M. Fitzgerald, K. Brown, and F. Osterwisch, AInfraredborne Scanning Spectrometer for Remote Sensing of Cloud, Aerosol, Water Vapor and Surface Properties, *JAOT*, submitted, 1995.
- Knowles, D., S.Y. Qiu, H. Montgomery, F. Chen, ATBD 1996 Thermal Calibration Algorithm: Detailed Support Document, MCST G031. Oct 1996, General Sciences Corporation, .
- Kurucz, R.L., Solar Flux Atlas from 296 to 1300 nm, National Solar Observatory, 1984.

McClain, C.R., W. Esaias, W. Barnes, B. Guenther, D. Endres, S.B. Hooker, B.G. Mitchell, and R. Barnes, Calibration and Validation Plan for SeaWiFS, NASA TM 104566, Vol 3, September 1992.

Mehrten, J., MODIS EM Temperature Telemetry Equations & Limits, SBRC, 1995.

Pagano, T., Gain Coefficients for Radiometric Calibration: version 2, SBRC, 1993.

Parker, K., and E. Knight, MODIS Operations Concept Document, GSFC, Greenbelt MD, 1995.

Rao, Degradation of the visible and near-infrared channels of the advanced very high resolution radiometer on the NOAA-9 spacecraft: assessment and recommendations for corrections, NOAA, 1993.

Salomonson, V.V., Team Leader Working Agreement for MODIS between the EOS AM & PM Projects at Goddard Space Flight Center and the MODIS Science Team Leader, Vincent V. Salomonson, of Goddard Space Flight Center, Goddard Space Flight Center, Greenbelt MD, 1994.

SBRS, Operational In-Flight Calibrations Procedures, CDRL 404, Hughes Santa Barbara Research Center, Santa Barbara California, 1993.

SBRS, Moderate Resolution Imaging Spectroradiometer (MODIS) Program Calibration Management Plan, SBRC, Goleta, California, 1994a.

SBRS, SBRC Critical Design Review Vol. III, 1994b.

Seber, G.A.F., *Linear Regression Analysis*, Wiley, 1977.

Slater, P.N., S.F. Biggar, R.G. Holm, R.D. Jackson, Y. Mao, M.S. Moran, J.M. Palmer, and B. Tuan, Reflectance and Radiance Based Methods for the in-flight Absolute Calibration of Multispectral Sensors, *Remote sensing of Environment*, 22, 11-37, 1987.

Slater, P., B. Biggar, K. Thome, Gellman, D., and P. Spyak, Vicarious Radiometric Calibrations of EOS Sensors, *J. Atmos. Ocean. Tech.*, 1996.

Team, M.S., M.C.S. Team, M.S.D.S. Team, S.B.R. Center, and U.S.G.S. (Flagstaff), The MODIS Calibration Plan Version 1.1, GSFC, 1994.

Veiga, R., H. Montgomery, and M. Jones, MODIS Solar Reflective Band Calibration Algorithm, MCST Ref. No. G028, September 1996.

Veiga, R., H. Montgomery, and M. Jones, Solar Diffuser and Solar Diffuser Stability Monitor In-Flight Calibration Algorithm Implementation, General Sciences Corporation, Seabrook Maryland, 1995.

Weber, S.R., Specification for the Moderate-Resolution Imaging Spectroradiometer (MODIS), GSFC, Greenbelt Maryland, 1993.

Wehrli, C. Extraterrestrial Solar Spectrum, World Radiation Center (WRC), Davos-Dorf, Switzerland, WRC Publication No. 615, July 1985.

Wolfe, R., J. Storey, E. Masuoka, and A. Fleig, MODIS Level 1A Earth Location Algorithm Theoretical Basis Document, NASA Goddard Space Flight Center, Greenbelt MD, 1995.

Young, J. B., SRCA along track SBR Modeling/algorithm, PL3095-N4214, August 24, 1995.

Young, J. B., SRCA Spectral Calibration Methodology, PL3095-N04744, March 20, 1995.

10. APPENDIX F: LEVEL 1B OUTPUT FILE SPECIFICATION

The five types of metadata are Core, Archive, Product, Swath, and SDS. The Core, Archive and Product metadata are stored as global attributes and the Swath metadata is stored as Vdata. The SDS metadata is stored as Science Data Set (SDS) attributes. The standard core granule metadata is the same for the three resolutions: 250m, 500m, and 1000m.

Global Metadata

ECS Standard Core Granule Metadata	
Stored as One ECS PVL String in :coremetadata.0=Global Attribute	
Description	Example
SHORTNAME	"MOD02"
VERSIONID	"2.0"
SIZEMBECSDATAGRANULE	400. (Obtained from system at runtime)
EASTBOUNDINGCOORDINATE	40.000000
WESTBOUNDINGCOORDINATE	15.000000
NORTHBOUNDINGCOORDINATE	25.000000
SOUTHBOUNDINGCOORDINATE	10.000000
EXCLUSIONGRINGFLAG.1	"N"
GRINGPOINTLATITUDE.1	(25.000000, 20.000000, 10.000000, 15.000000)
GRINGPOINTLONGITUDE.1	(20.000000, 40.000000, 35.000000, 15.000000)
GRINGPOINTSEQUENCENO.1	(1, 2, 3, 4)
ORBITNUMBER	1234
RANGEBEGINNINGDATETIME	"2002-02-23T11:02:27.987654Z"
RANGEENDINGDATETIME	"2002-02-23T11:04:57.987654Z"
QAPERCENTINTERPOLATEDDATA	0
QAPERCENTOUTOFBOUNDSDATA	0
QAPERCENTMISSINGDATA	0
AUTOMATICQUALITYFLAG	"passed"
OPERATIONALQUALITYFLAG	"not being investigated"
SCIENCEQUALITYFLAG	"not being investigated"
QUALITYFLAGEXPLANATION	"not being investigated"
REPROCESSINGACTUAL	"processed once"
REPROCESSINGPLANNED	"no further update anticipated"
INPUTPOINTER	"LIA and Geolocation file name(s), Reflective.LUT, Emissive.LUT, sd.coeff.trend "
OPERATIONMODE	"day"

The archive granule metadata is the same for the three resolutions: 250m, 500m, and 1000m.

MODIS Level 1B Archive Granule Metadata Stored as HDF ECS PVL in :ArchiveMetadata.0=Global Attribute	
Description	Example
PROCESSINGDATETIME	"2002-02-23T11:04:57.987654Z"
SPSOPARAMETERS	"The SPSO parameters (see database) for all data contained in this file"
ALGORITHMPACKAGEACCEPTANCEDATE	"1997-01-01"
ALGORITHMPACKAGEMATURITYCODE	"pre-launch"
ALGORITHMPACKAGENAME	"MOD02V2.0"
ALGORITHMPACKAGEVERSION	"version 2.0"
INSTRUMENTNAME	"Moderate-Resolution Imaging SpectroRadiometer"
PLATFORMSHORTNAME	"EOS AM1"
PROCESSINGCENTER	"GSFC"
ROUTINEINSTRUMENTOPERATIONS	"Y" or "N"
CALIBRATIONDATAQUALITY	"good", "marginal" OR "bad"
NADIRPOINTING	"Y" or "N"
MISSIONPHASE	"A&E" OR "post A&E"

The archive granule metadata is the same for the three resolutions: 250m, 500m, and 1000m.

MODIS Level 1B Product Granule Metadata Stored as Native HDF Global Attributes		
Description	Format	Example
"Number of Scans"	Int32	203
"Number of Day mode scans"	Int32	203
"Number of Night mode scans"	Int32	0
"Incomplete Scans"	Int32	14
"Max Earth View Frames"	Int32	1354
"% Valid EV Observations"	float32[38]	98.2,..., 87.1,...,46.0,...
"% Saturated EV Observations"	float32[38]	1.4,..., 0.2,...,7.9,...
"Post Processing Indicates Bad data"	Int32[38]	1=True; 0=False
"Electronics Redundancy Vector"	Int64	One bit set to 0 for Side A or 1 for Side B, for each programmable component
"Reflective LUT Last Change Date"	string	"1997-02-28T00:00:00"
"Emissive LUT Last Change Date"	string	"1997-02-28T00:00:00"
"Focal Plane Set Point State"	Int8[4]	0=Running open loop 1=Set Point is 83 degrees 2=Set Point is 85 degrees 3=Set Point is 88 degrees

DataField_15, "Height", DFNT_INT16,	("2*nscans", "Max_EV_frames/5")
DataField_16, "SensorZenith", DFNT_INT16,	("2*nscans", "Max_EV_frames/5")
DataField_17, "SensorAzimuth", DFNT_INT16,	("2*nscans", "Max_EV_frames/5")
DataField_18, "Range", DFNT_INT16,	("2*nscans", "Max_EV_frames/5")
DataField_19, "SolarZenith", DFNT_INT16,	("2*nscans", "Max_EV_frames/5")
DataField_20, "SolarAzimuth", DFNT_INT16,	("2*nscans", "Max_EV_frames/5")
DataField_21, "gflags", DFNT_INT8,	("2*nscans", "Max_EV_frames/5")

For the 250m bands the Swath Metadata has the form

Level 1B HDF-EOS Swath Metadata Stored as HDF ECS PVL in :StructMetadata.0=Global Attribute
<pre> GROUP=SwathStructure GROUP=SWATH_1 SwathName="MODIS_Swath_Type_L1B" GROUP=Dimension Dimension_1, "Band_250M", Size=2 Dimension_2, "10*nscans", Size=10*nscans Dimension_3, "40*nscans", Size=40*nscans Dimension_4, "Max_EV_frames", Size=Max_EV_frames Dimension_5, "4*Max_EV_frames", Size=4*Max_EV_frames GROUP=DimensionMap DimensionMap_1, GeoDimension="10*nscans", DataDimension="40*nscans", Offset=3, Increment=4 DimensionMap_2, GeoDimension=" Max_EV_frames", DataDimension=" 4*Max_EV_frames", Offset=1, Increment=4 GROUP=GeoField GeoField_1, "Latitude", DFNT_FLOAT32, ("10*nscans","Max_EV_frames") GeoField_2, "Longitude", DFNT_FLOAT32, ("10*nscans","Max_EV_frames") GROUP=DataField DataField_1, "Band_250M", DFNT_FLOAT32, ("Band_250M") DataField_2, "EV_250_RefSB", DFNT_UINT16, ("Band-250M", "40*nscans", "4*Max_EV_frames") DataField_3, "EV_250M_RefSB_Uncert_Indexes", DFNT_UINT16, ("Band_250M", "40*nscans", "4*Max_EV_frames") </pre>

The Vdata is the same for the 250m, 500m, and 1000m bands

"Level 1B Specific Swath Metadata"		
Written as Vdata with the Following Fields		
Field	Type	Typical value
Scan Number	int32	Range 1 to 100
Complete Scan Flag	int32	Complete=1, Incomplete=0
Scan Type	char8[4]	"D "=day, "N "=night, "M "=mixed, "O "=other
Mirror Side	int32	1 or 2
EV Sector Start Time	float64	TAI: Sec. since midnight 1/1/93
Programmed_EV_Frames	int32	1514
EV_Frames	int32	1354
Nadir_Frame_Number	int32	677
Latitude of Nadir Frame	float32	-90.0 to 90.0 in degrees
Longitude of Nadir Frame	float32	-180.0 to 180.0 in degrees
Solar Azimuth of Nadir Frame	float32	-180 to 180 degrees
Solar Zenith of Nadir Frame	float32	0.0 to 180.0 in degrees
No. thermistor outliers	int32	Range 0 to 12
Bit QA Flags	int32	1=True; 0=False
Moon in SV Port	bit 0	
Spacecraft Maneuver	bit 1	
Sector Rotation	bit 2	
Negative Radiance Beyond Noise Level	bit 3	
PC Ecal on	bit 4	
PV Ecal on	bit 5	
SD Door Open	bit 6	
SD Screen Down	bit 7	
SRCA On	bit 8	
SDSM On	bit 9	
Outgassing	bit 10	
Instrument Standby Mode	bit 11	
Linear Emissive Calibration	bit 12	
DC Restore Change	bit 13	
BB/Cavity Temperature Differential	bit 14	
BB Heater On	bit 15	
Missing Previous Granule	bit 16	
Missing Subsequent Granule	bit 17	
Remaining 14 bits reserved for future use	bits 18 - 31	

Band Subsetting SDSs		
SDS Name	Data Type	HDF Dimension Names
"Band_250M"	float32	floating point array of dimension (Band_250M)
<p>Band_250M SDS Attributes: long_name = "250M Band Numbers for Subsetting" Note: The values stored in this array are 1.0 and 2.0 Band_250M Dimension Attributes: band_names = "1, 2" radiance_scales = x.f, x.f radiance_offsets = x.f, x.f radiance_units = "Watts/m²/μm/steradian" reflectance_scales = x.f, x.f reflectance_offsets = x.f, x.f reflectance_units = "1/steradian" corrected_counts_scales = x.f, x.f corrected_counts_offsets = x.f, x.f corrected_counts_units = "counts"</p>		
"Band_500M"	float32	floating point array of dimension (Band_250M)
<p>Band_500M SDS Attributes: long_name = "500M Band Numbers for Subsetting" Note: The values stored in this array are 3.0, 4.0, 5.0, 6.0, and 7.0 Band_500M Dimension Attributes: band_names = "3, 4, 5, 6, 7" radiance_scales = x.f, x.f, x.f, x.f, x.f radiance_offsets = x.f, x.f, x.f, x.f, x.f radiance_units = "Watts/m²/μm/steradian" reflectance_scales = x.f, x.f, x.f, x.f, x.f reflectance_offsets = x.f, x.f, x.f, x.f, x.f reflectance_units = "1/steradian" corrected_counts_scales = x.f, x.f, x.f, x.f, x.f corrected_counts_offsets = x.f, x.f, x.f, x.f, x.f corrected_counts_units = "counts"</p>		

Band Subsetting SDSs		
SDS Name	Data Type	HDF Dimension Names
"Band_1KM_RefSB "	float32	floating point array of dimension (Band_1KM_RefSB)
<p>Band_1KM_RefSB SDS Attributes: long_name = "1KM Reflective Solar Band Numbers for Subsetting" Note: The values stored in this array are 8.0, 9.0, 10.0, 11.0, 12.0, 13.0, 13.5, 14.0, 14.5, 15.0, 16.0, 17.0, 18.0, 19.0 and 26.0 Band_1KM_RefSB Dimension Attributes: band_names = "8, 9, 10, 11, 12, 13lo, 13hi, 14lo, 14hi, 15, 16, 17, 18, 19, 26" radiance_scales = x.f, x.f radiance_offsets = x.f, x.f radiance_units = "Watts/m²/μm/steradian" reflectance_scales = x.f, x.f reflectance_offsets = x.f, x.f reflectance_units = "1/steradian" corrected_counts_scales = x.f, x.f corrected_counts_offsets = x.f, x.f corrected_counts_units = "counts"</p>		
"Band_1KM_Emissive "	float32	floating point array of dimension (Band_1KM_Emissive)
<p>Band_1KM_Emissive SDS Attributes: long_name = "1KM Emissive Band Numbers for Subsetting" Note: The values stored in this array are 20.0, 21.0, 22.0, 23.0, 24.0, 25.0, 27.0, 28.0, 29.0, 30.0, 31.0, 32.0, 33.0, 34.0, 35.0, 36.0 Band_1KM_Emissive Dimension Attributes: band_names = "20, 21, 22, 23, 24, 25, 27, 28, 29, 30, 31, 32, 33, 34, 35, 36" radiance_scales = x.f, x.f radiance_offsets = x.f, x.f radiance_units = "Watts/m²/μm/steradian" corrected_counts_scales = x.f, x.f, x.f corrected_counts_offsets = x.f, x.f, x.f corrected_counts_units = "counts"</p>		

Band Subsetting SDS

"Band_250M(Band_250M)"	int16	Band_250M = 2
Band_250M SDS Attributes: long_name = "250M Band Numbers for Subsetting" Note: The values stored in this array are 1.0 and 2.0 Band_250M Dimension Attributes: band_names = "1, 2" radiance_scales = x.f, x.f radiance_offsets = x.f, x.f radiance_units = "Watts/m ² /μm/steradian" reflectance_scales = x.f, x.f reflectance_offsets = x.f, x.f reflectance_units = "1/steradian" corrected_counts_scales = x.f, x.f corrected_counts_offsets = x.f, x.f corrected_counts_units = "counts"		

Instrument and Uncertainty SDSs
--

SDS Name	Data Type	HDF Dimension Names
"EV_250_Aggr1km_RefSB"	uint16	16 bit scaled integer array of dimension (Band_250M, 10*nscans, Max_EV_frames)
EV_250_Aggr1km_RefSB SDS Attributes: long_name = "Earth View 250M Aggregated 1km Reflected Solar Bands Scaled Integers" Band_250M Dimension Attributes: band_names = "1, 2" radiance_scales = x.f, x.f radiance_offsets = x.f, x.f radiance_units = "Watts/m ² /μm/steradian" reflectance_scales = x.f, x.f reflectance_offsets = x.f, x.f reflectance_units = "1/steradian" corrected_counts_scales = x.f, x.f corrected_counts_offsets = x.f, x.f corrected_counts_units = "counts"		
"EV_250_Aggr1km_RefSB_UncertIndexes"	uint8	8 bit integer array of dimension (Band_250M, 10*nscans, Max_EV_frames)
EV_250_Aggr1km_RefSB_Uncert_Indexes SDS Attributes: long_name = "Earth View 250M Aggregated 1km Reflected Solar Bands Uncertainty Indexes"		

Instrument and Uncertainty SDSs		
SDS Name	Data Type	HDF Dimension Names
"EV_250_Aggr1km_RefSB_Samples_Used"	int8	8 bit integer array of dimension (Band_250M, 10*nscans, Max_EV_frames)
EV_250_Aggr1km_RefSB_Samples_Used SDS Attributes: long_name = "Earth View 250M Aggregated 1km Reflected Solar Bands Number of Samples Used in Aggregation"		
"EV_250_RefSB "	Unsigned Integer (16 bits)	16 bit scaled integer array of dimension (Band_250M, 40*nscans, 4*EV_frames)
EV_250_RefSB SDS Attributes: long_name = "Earth View 250M Reflected Solar Bands Scaled Integers" Band_250M Dimension Attributes: band_names = "1, 2" radiance_scales = x.f, x.f radiance_offsets = x.f, x.f radiance_units = "Watts/m ² /μm/steradian" reflectance_scales = x.f, x.f reflectance_offsets = x.f, x.f reflectance_units = "1/steradian" corrected_counts_scales = x.f, x.f corrected_counts_offsets = x.f, x.f corrected_counts_units = "counts"		
"EV_250_RefSB_Uncert_Indexes"	Int8	8 bit integer array of dimension (Band_250M, 40*nscans, 4*EV_frames)
EV_250_RefSB_Uncert_Indexes SDS Attributes: long_name = "Earth View 250M Reflected Solar Bands Uncertainty Indexes"		
"EV_250_Aggr500_RefSB"	uint16	16 bit scaled integer array of dimension (Band_250M, 20*nscans, 2*EV_frames)
EV_250_Aggr500_RefSB SDS Attributes: long_name = "Earth View 250M Aggregate 500M Reflected Solar Bands Scaled Integers" Band_250M Dimension Attributes: band_names = "1, 2" radiance_scales = x.f, x.f radiance_offsets = x.f, x.f radiance_units = "Watts/m ² /μm/steradian" reflectance_scales = x.f, x.f reflectance_offsets = x.f, x.f reflectance_units = "1/steradian" corrected_counts_scales = x.f, x.f corrected_counts_offsets = x.f, x.f corrected_counts_units = "counts"		

Instrument and Uncertainty SDSs		
SDS Name	Data Type	HDF Dimension Names
"EV_250_Aggr500_RefSB_Uncert_Indexes"	Int8	8 bit integer array of dimension (Band_250M, 20*nscans, 2*Max_EV_frames)
EV_250_Aggr500_RefSB_Uncert_Indexes SDS Attributes: long_name = "Earth View 250M Aggregate 500M Reflected Solar Bands Uncertainty Indexes"		
"EV_500_RefSB"	uint16	16 bit scaled integer array of dimension (Band_500M, 20*nscans, 2*Max_EV_frames)
EV_500_RefSB SDS Attributes: long_name = "Earth View 500M Reflected Solar Bands Scaled Integers" Band_500M Dimension Attributes: band_names = "3, 4, 5, 6, 7" radiance_scales = x.f, x.f, x.f, x.f, x.f radiance_offsets = x.f, x.f, x.f, x.f, x.f radiance_units = "Watts/m ² /μm/steradian" reflectance_scales = x.f, x.f, x.f, x.f, x.f reflectance_offsets = x.f, x.f, x.f, x.f, x.f reflectance_units = "1/steradian" corrected_counts_scales = x.f, x.f, x.f, x.f, x.f corrected_counts_offsets = x.f, x.f, x.f, x.f, x.f corrected_counts_units = "counts"		
"EV_500_RefSB_Uncert_Indexes"	Int8	8 bit integer array of dimension (Band_500M, 20*nscans, 2*Max_EV_frames)
EV_500_RefSB_Uncert_Indexes SDS Attributes: long_name = "Earth View 500M Reflected Solar Bands Uncertainty Indexes"		
"EV_500_Aggr1km_RefSB"	uint16	16 bit scaled integer array of dimension (Band_500M, 10*nscans, Max_EV_frames)
EV_500_RefSB SDS Attributes: long_name = "Earth View 500M Aggregated 1km Reflected Solar Bands Scaled Integers" Band_500M Dimension Attributes: band_names = "3, 4, 5, 6, 7" radiance_scales = x.f, x.f, x.f, x.f, x.f radiance_offsets = x.f, x.f, x.f, x.f, x.f radiance_units = "Watts/m ² /μm/steradian" reflectance_scales = x.f, x.f, x.f, x.f, x.f reflectance_offsets = x.f, x.f, x.f, x.f, x.f reflectance_units = "1/steradian" corrected_counts_scales = x.f, x.f, x.f, x.f, x.f corrected_counts_offsets = x.f, x.f, x.f, x.f, x.f corrected_counts_units = "counts"		

Instrument and Uncertainty SDSs		
SDS Name	Data Type	HDF Dimension Names
"EV_500_Aggr1km_RefSB_Uncert_Indexes"	uint8	8 bit integer array of dimension (Band_500M, 10*nscans, Max_EV_frames)
EV_500_RefSB_Uncert_Indexes SDS Attributes: long_name = "Earth View 500M Aggregated 1km Reflected Solar Bands Uncertainty Indexes"		
"EV_500_Aggr1km_RefSB_B_Samples_Used"	int8	8 bit integer array of dimension (Band_500M, 10*nscans, Max_EV_frames)
EV_500_Aggr1km_RefSB_Samples_Used SDS Attributes: long_name = "Earth View 500M Aggregated 1km Reflected Solar Bands Number of Samples Used in Aggregation"		
"EV_1000_RefSB"	uint16	16 bit scaled integer array of dimension (Band_1KM_RefSB, 10*nscans, Max_EV_frames)
EV_1000_RefSB SDS Attributes: long_name = "Earth View 1KM Reflected Solar Bands Scaled Integers" Band_1KM_RefSB Dimension Attributes: band_names = "8, 9, 10, 11, 12, 13lo, 13hi, 14lo, 14hi, 15, 16, 17, 18, 19, 26" radiance_scales = x.f, x.f radiance_offsets = x.f, x.f radiance_units = "Watts/m ² /μm/steradian" reflectance_scales = x.f, x.f reflectance_offsets = x.f, x.f reflectance_units = "1/steradian" corrected_counts_scales = x.f, x.f corrected_counts_offsets = x.f, x.f corrected_counts_units = "counts"		
"EV_1000_RefSB_Uncert_Indexes"	uint8	8 bit integer array of dimension (Band_1KM_RefSB, 10*nscans, Max_EV_frames)
EV_1000_RefSB_Uncert_Indexes SDS Attributes: long_name = "Earth View 1KM Reflected Solar Bands Uncertainty Indexes"		
"EV_1000_Emissive"	uint16	16 bit scaled integer array of dimension (Band_1KM_Emissive, 10*nscans, Max_EV_frames,)
EV_1000_Emissive SDS Attributes: long_name = "Earth View 1KM Emissive Bands Scaled Integers" Band_1KM_Emissive Dimension Attributes: band_names = "20, 21, 22, 23, 24, 25, 27, 28, 29, 30, 31, 32, 33, 34, 35, 36" radiance_scales = x.f, x.f radiance_offsets = x.f, x.f radiance_units = "Watts/m ² /μm/steradian" corrected_counts_scales = x.f, x.f corrected_counts_offsets = x.f, x.f corrected_counts_units = "counts"		

Instrument and Uncertainty SDSs		
SDS Name	Data Type	HDF Dimension Names
"EV_1000_Emissive_Uncert_Indexes"	uint8	8 bit integer array of dimension (Band_1KM_Emissive, 10*nscans, Max_EV_frames,)
EV_1000_Emissive_Uncert_Indexes SDS Attributes: long_name = "Earth View 1KM Emissive Bands Uncertainty Indexes"		

Geolocation SDSs		
SDS Name	Data Type	HDF Dimension Names
"Latitude"	float32	32 bit floating point array of dimension (2*nscans, Max_EV_frames/5)
Latitude SDS Attributes: units = degrees valid_range = -180.0, 180.0 _FillValue = -999.9 line_numbers = [3, 8] frame_numbers = [3, 8, 13,...]		
"Longitude"	float32	32 bit floating point array of dimension (2*nscans, Max_EV_frames/5)
Longitude SDS Attributes: units = degrees valid_range = -90.0, 90.0 _FillValue = -999.9 line_numbers = [3, 8] frame_numbers = [3, 8, 13,...]		
"Height"	int16	16 bit integer array of dimension (2*nscans, Max_EV_frames/5)
Height SDS Attributes: units = meters valid_range = 0, 10000 _FillValue = -32767 line_numbers = [3, 8] frame_numbers = [3, 8, 13,...] scale_factor = 0.01		

Geolocation SDSs		
SDS Name	Data Type	HDF Dimension Names
"SensorZenith"	int16	16 bit integer array of dimension (2*nscans, Max_EV_frames/5)
SensorZenith SDS Attributes: units = degrees valid_range = 0, 15730 _FillValue = -32767, 32767 line_numbers = [3, 8] frame_numbers = [3, 8, 13,...] scale_factor = 0.01		

Geolocation SDSs		
SDS Name	Data Type	HDF Dimension Names
"SensorAzimuth"	int16	16 bit integer array of dimension (2*nscans, Max_EV_frames/5)
SensorAzimuth SDS Attributes: units = degrees valid_range = -3146 line_numbers = [3, 8] frame_numbers = [3, 8, 13,...] scale_factor = 0.01		

"Range"	uint16	16 bit unsigned integer array of dimension (2*nscans, Max_EV_frames/5)
Range SDS Attributes: units = meters valid_range = 27000,65535 _FillValue = 0 line_numbers = [3, 8] frame_numbers = [3, 8, 13,...] scale_factor = 50		

"SolarZenith"	int16	16 bit integer array of dimension (2*nscans, Max_EV_frames/5)
SolarZenith SDS Attributes: units = degrees valid_range = 0, 31460 _FillValue = -32767 line_numbers = [3, 8] frame_numbers = [3, 8, 13,...] scale_factor = 0.01		

Geolocation SDSs		
SDS Name	Data Type	HDF Dimension Names
"SolarAzimuth"	int16	16 bit integer array of dimension (2*nscans, Max_EV_frames/5)
SolarAzimuth SDS Attributes: units = degrees valid_range = -31460, 31460 _FillValue = -32767 line_numbers = [3, 8] frame_numbers = [3, 8, 13,...] scale_factor = 0.01		
"gflags"	int8	8 bit integer array of dimension (2*nscans, Max_EV_frames/5)
gflags SDS Attributes: Bit 0: 1 = invalid input data Bit 1: 1 = no ellipsoid intersection Bit 2: 1 = no valid terrain data Bit 3: 1 = invalid sensor angles Bit 4: 1 = invalid solar angles		

11. APPENDIX G: SPURIOUS RADIANCE CONTRIBUTION SOURCES SUMMARY

Nominal Scene	Cavity Emission Sources [$L_{emiss}(T_{cav})$]	Earth Scene Sources $L_{scene_refl}(T_{scene})$	
Earth View	1) Earth Aperture Surround Emission scattered into FOV. Estimated to be nil from Cavity Scatter model.	Scene Scatter	2) MODIS fore-optics and aft-optics will scatter radiances according to scene contrast details. Near-Field and Far-Field scatter are not included in LIB algorithm
		Cavity Reflections	3) Potential spurious reflections from cavity surfaces and scan mirror edges. Estimated to be nil .
		Fold Mirror Scatter	4) Fold Mirror scatter of Earth scene viewed directly by the Fold Mirror. Estimated to be nil .
Space View	1) Space View Surround , Emission scattered into FOV. Value estimation is in Ref	Cavity Reflections	2) Potential spurious reflections from cavity surfaces and scan mirror edges. Estimated to be nil .
		Fold Mirror Scatter	3) Fold Mirror scatter of Earth scene viewed directly by the Fold Mirror. Estimated to be nil .
Blackbody View	1) Cavity emission scattered via Scan Mirror into FOV. 2) Cavity emission reflected via blackbody into FOV	BB Reflections of Scene	2) Two distinct BB specular reflection paths from two localized Earth scene regions (+33°; -58° from nadir), and whole scene reflection paths from BB teeth imperfection.
		Cavity Reflections	3) Potential spurious reflections from cavity surfaces and scan mirror edges Estimated to be nil .
		Fold Mirror Scatter	4) Fold Mirror scatter of Earth scene viewed directly by the Fold Mirror. Estimated to be nil .